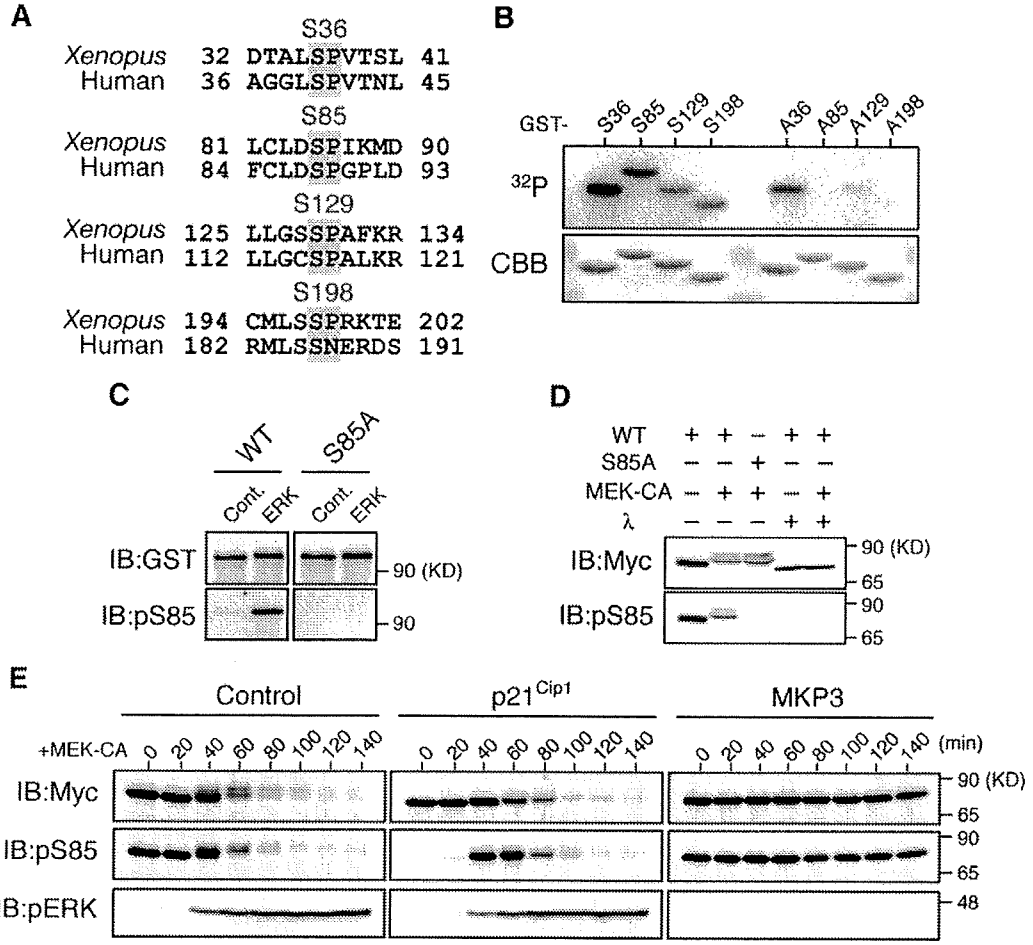

Figure 3. Phosphorylation of Xe-Cdc25A by ERK. (A) Conservation of consensus ERK phosphorylation motifs (Ser-Pro) in *Xenopus* and human Cdc25A proteins. (B) The indicated GST-fused Xe-Cdc25A peptides were incubated with [γ-^{32}P]ATP and ERK protein and analyzed as described in Figure 2B. (C) GST-tagged full-length Xe-Cdc25A proteins (WT or S85A) were synthesized in wheat germ extracts, purified by GST-pull-down, incubated with either buffer (Cont.) or ERK protein, and analyzed by immunoblotting with anti-GST and anti-phospho-S85 antibodies. (D) Activated eggs were injected with 2 ng of mRNA encoding Myc-Xe-Cdc25A (WT or S85A), reinjected or not 2.5 h later with 9 ng of MEK-CA mRNA, and cultured for 50 min. Egg extracts were treated or not with λ-phosphatase and analyzed for Myc-Xe-Cdc25A and phospho-S85 by immunoblotting. (E) Activated eggs were injected with either buffer (Control), 18 ng of p21^{Cip1} mRNA, or 9 ng of MKP3 mRNA, reinjected 40 min later with 2 ng of Myc-Xe-Cdc25A mRNA, further injected 2.5 h later with 9 ng of MEK-CA mRNA, collected at the indicated times, and analyzed by immunoblotting as described in D. Four, three, four, and five independent experiments were performed for B, C, D, and E, respectively, and, for each, a typical result is shown.

inhibited by ERK inactivation by MKP3 (Figure 1D). Interestingly, Xe-Cdc25A has four Ser residues (S36, S85, S129, and S198) that lie in the ERK consensus phosphorylation motif (Ser/Thr-Pro) and are mostly conserved in human Cdc25A (Figure 3A). Therefore, we first examined whether these four Ser residues could be phosphorylated by ERK in vitro, using [γ-^{32}P]ATP and GST-fused Xe-Cdc25A peptides, essentially as performed earlier for p90rsk (Figure 2B). As shown in Figure 3B, ERK was able to phosphorylate all of the four Ser residues, particularly S85, in vitro.

Because S85 and its equivalent site S88 are required for the Chk1-induced degradations of Xe-Cdc25A and human Cdc25A, respectively (Busino *et al.*, 2003; Kanemori *et al.*, 2005), we investigated S85 phosphorylation by ERK in more detail. When phosphorylated by ERK in vitro, GST-fused full-length Xe-Cdc25A WT, but not its S85A mutant, was efficiently recognized by anti-phospho-S85 antibody (Figure 3C), confirming that S85 of Xe-Cdc25A can be phosphorylated by ERK in vitro. We then analyzed S85 phosphorylation in vivo. When coexpressed with MEK-CA in activated eggs, Xe-Cdc25A WT, but not the S85A mutant, was recognized by the anti-phospho-S85 antibody in a manner sensitive to λ-phosphatase treatment (Figure 3D). Surprisingly, however, S85 phosphorylation was detected even in the absence of MEK-CA expression (Figure 3D; see also time 0 in Figure 3E, Cont.) and after MEK-CA expression in the presence of pre-expressed MKP3 (Figure 3E, MKP3). Interestingly, this unexpected phosphorylation was strongly inhibited by prior expression of the Cdk inhibitor p21^{Cip1} (see times 0 and 20 min in Figure 3E, p21^{Cip1}), indicating that it was mediated by Cdk, another proline-directed kinase. Importantly, however, despite the presence of p21^{Cip1}, S85 phosphorylation did occur concurrently with ERK activation (and during Xe-Cdc25A degradation) after MEK-CA expression (see times 40–80 min in Figure 3E, p21^{Cip1}); this result was even clearer when the stable D231A mutant,

instead of the WT, was used for the analysis (Supplemental Figure S1A). Thus, these results show that ERK can directly phosphorylate Xe-Cdc25A on S85 both in vitro and in vivo and also on S36, S129, and S198 at least in vitro.

Contribution of ERK-catalyzed Phosphorylation to Xe-Cdc25A Degradation

To examine the requirement of ERK-catalyzed phosphorylations for Xe-Cdc25A degradation, we constructed several Xe-Cdc25A mutants, i.e., four single-Ala mutants (S36A, S85A, S129A, and S198A) and one quadruple-Ala mutant (S36/85/129/198A, termed SP:4A), and expressed them in activated eggs. After MEK-CA expression, the S129A mutant was as unstable as the WT, but both the S36A and S198A mutants were slightly more stable than the WT, and both the S85A and SP:4A mutants were significantly more stable than the WT (Figure 4A). In addition, reversion of Ala-129 to Ser (in SP:4A) had no appreciable effect on the stability of the SP:4A mutant, but reversion of Ala-36, Ala-85, or Ala-198 to Ser, particularly that of Ala-85 to Ser, significantly destabilized the SP:4A mutant (Figure 4B). Thus, these results suggest that most of the ERK-catalyzed phosphorylations, particularly phosphorylation at S85, contribute to the MEK-CA–induced degradation of Xe-Cdc25A.

As for S85 phosphorylation, this phosphorylation was probably mediated in part by Cdk (Figure 3E, $p21^{Cip1}$; Supplemental Figure S1A). However, even without Cdk activity (or in the presence of $p21^{Cip1}$), ERK activation was able to efficiently induce the degradation of Xe-Cdc25A WT (Figure 3E, $p21^{Cip1}$) but not of the S85A mutant (Supplemental Figure S1B). Thus, although Cdk also phosphorylates S85, ERK-catalyzed S85 phosphorylation alone is sufficient for the S85 phosphorylation-dependent degradation of Xe-Cdc25A.

We also compared stabilities of the SP:4A mutant, the p90rsk phosphorylation site mutant (RXXS:4A), the RXXS:4A/SP:4A double mutant (8A), and the β-TrCP binding site mutant (D231A) after MEK-CA expression. The SP:4A mutant was somewhat less stable than the completely stable D231A mutant (Figure 4C). The RXXS:4A mutant was also somewhat less stable than the D231A mutant (Figure 4C), consistent with earlier results (Figure 2A). However, the double 8A mutant was very stable, comparable with the D231A mutant (Figure 4C). Thus, these results strongly suggest that ERK phosphorylation and p90rsk phosphorylation contribute, roughly equally and additively, to the MEK-CA–induced degradation of Xe-Cdc25A. Significantly, by similar analyses, we also obtained evidence that ERK and p90rsk phosphorylations can target human Cdc25A for $SCF^{\beta\text{-}TrCP}$-dependent degradation in activated *Xenopus* eggs (Supplemental Figure S2).

ERK Pathway-dependent Degradation of Xe-Cdc25A during Oocyte Maturation

Given our results, Cdc25A might be degraded in an $SCF^{\beta\text{-}TrCP}$-dependent manner under physiological conditions in which the endogenous ERK pathway is strongly activated. During oocyte maturation in many species, the endogenous ERK pathway becomes fully activated under the control of Mos (which activates MEK) and plays an important role for meiotic division of the oocyte (Sagata, 1997; Kishimoto, 2003). Interestingly, a recent study in mice showed that Cdc25A present in immature oocytes is degraded during oocyte maturation, although the degradation mechanism is not known (Solc *et al.*, 2008). We therefore asked whether Xe-Cdc25A could be degraded in an $SCF^{\beta\text{-}TrCP}$- and ERK pathway-dependent manner during *Xenopus* oocyte maturation. Somewhat surprisingly, unlike in mice (Solc *et al.*, 2008),

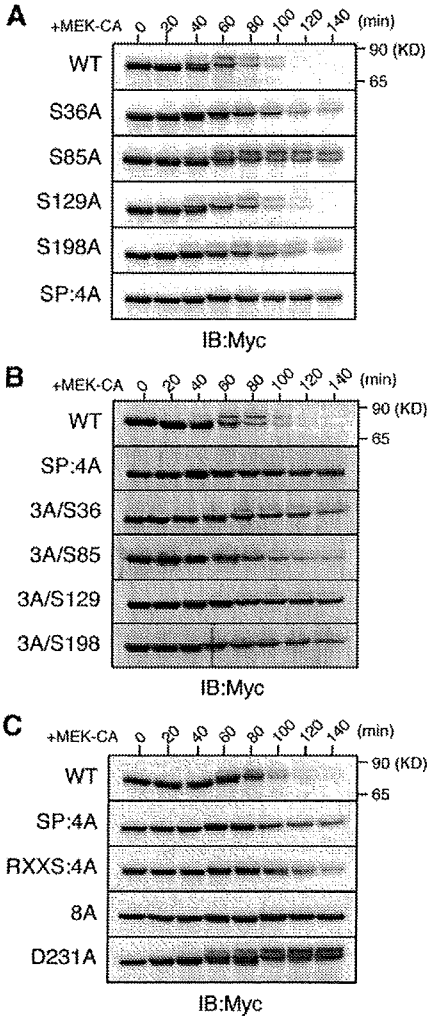

Figure 4. Requirement of ERK phosphorylation for Xe-Cdc25A degradation. (A–C) Activated eggs were injected with 2 ng of mRNA encoding the indicated Myc-Xe-Cdc25A constructs, reinjected 2.5 h later with 9 ng of MEK-CA mRNA, and analyzed for Myc-Xe-Cdc25A constructs by immunoblotting. In B, 3A/S36, etc., are reversion mutants of SP:4A (see text). Four independent experiments were performed for A–C, and, for each, a typical result is shown.

endogenous Xe-Cdc25A was not present in immature *Xenopus* oocytes, although it was present after fertilization, as reported previously (Kim *et al.*, 1999) (Figure 5A; also see Figure 1, A–C). Interestingly, however, ectopically expressed Xe-Cdc25A was readily detected in immature oocytes and was degraded during progesterone-induced oocyte maturation, coincidently with germinal vesicle breakdown (a hallmark for entry into meiosis I) (Figure 5B, Control) and ERK activation (Figure 5C, Control). Importantly, this degradation of Xe-Cdc25A was dependent on both $SCF^{\beta\text{-}TrCP}$ and ERK activity, because it was prevented either by overexpression of a dominant-negative mutant of β-TrCP (Figure 5B, β-TrCPΔF) or by treatment of the oocytes with the MEK-specific inhibitor U0126 (Figure 5C). Furthermore, and notably, both the RXXS:4A and SP:4A mutants were significantly more stable than Xe-Cdc25A WT, whereas both the double mutant (8A) and the β-TrCP-nonbinding

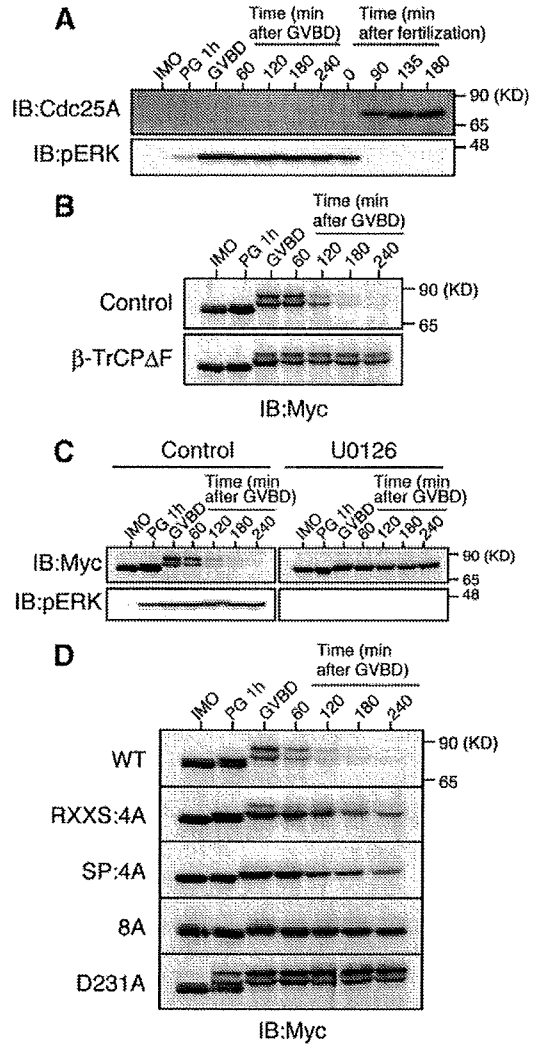

Figure 5. ERK pathway-dependent degradation of Xe-Cdc25A during oocyte maturation. (A) Immature oocytes (IMO) were treated with progesterone (PG) to induce maturation, whereas ovulated eggs were fertilized in vitro. Maturing oocytes and fertilized eggs were collected at the indicated times, and analyzed for endogenous Xe-Cdc25A and phospho-ERK by immunoblotting. GVBD denotes germinal vesicle breakdown. (B) Immature oocytes were coinjected with 2 ng of Myc-Xe-Cdc25A mRNA and 20 ng of either GST mRNA (Control) or β-TrCPΔF mRNA, cultured overnight, treated with progesterone, and analyzed for Myc-Xe-Cdc25A by immunoblotting. (C) Immature oocytes were injected with 2 ng of Myc-Xe-Cdc25A mRNA, cultured overnight, pretreated with dimethyl sulfoxide (Control) or 100 μM U0126 for 1 h, treated with progesterone, and analyzed for Myc-Xe-Cdc25A and phospho-ERK by immunoblotting. (D) Immature oocytes were injected with 2 ng of mRNA encoding the indicated Myc-Xe-Cdc25A constructs, cultured overnight, treated with progesterone, and analyzed for Myc-Xe-Cdc25A constructs by immunoblotting. In B–D, all the Myc-Xe-Cdc25A constructs were, in fact, phosphatase-dead C428S forms to avoid premature maturation of the oocytes. Four, three, four, and five independent experiments were performed for A, B, C, and D, respectively, and, for each, a typical result is shown.

mutant D231A were nearly completely stable, during oocyte maturation (Figure 5D). Additionally, the relative stabilities of these mutants during oocyte maturation were essentially the same as those observed in activated eggs expressing MEK-CA (compare Figures 4C and 5D). Thus, most probably, both ERK and p90rsk in the Mos–MEK–ERK–p90rsk pathway, as well as $SCF^{\beta\text{-}TrCP}$, are involved in the degradation of (ectopic) Xe-Cdc25A during oocyte maturation. These results suggest that, even under physiological conditions, a strongly activated ERK pathway can target coexisting Cdc25A for $SCF^{\beta\text{-}TrCP}$-dependent degradation.

Cell Cycle Arrest by ERK-induced Xe-Cdc25A Degradation

Cdc25A dephosphorylates Cdk1/Cdk2 on Thr-14/Tyr-15 residues and thereby promotes cell cycle progression in mammalian cells (Hoffmann *et al.*, 1994; Molinari *et al.*, 2000). Xe-Cdc25A begins to be synthesized after fertilization or egg activation (Figure 5A; Kim *et al.*, 1999) and is involved in the rapid embryonic cell cycles (Kim *et al.*, 1999). To determine whether ERK-induced Xe-Cdc25A degradation can elicit cell cycle arrest at interphase as does Chk1-induced Cdc25A degradation (Mailand *et al.*, 2000; Shimuta *et al.*, 2002; Busino *et al.*, 2003), we ectopically expressed MEK-CA in one-cell embryos, and then monitored the inhibitory T14/Y15 phosphorylation of Cdk1 as well as the external morphology of embryos (Shimuta *et al.*, 2002). In this experiment, however, we used embryos depleted of endogenous Erp1 (a maternal meiotic inhibitor) by antisense morpholino oligos (Figure 6A), because this maternal factor, if present and phosphorylated by p90rsk, induces metaphase arrest of the embryo owing to its cytostatic factor activity (Inoue *et al.*, 2007; Nishiyama *et al.*, 2007). Expression of MEK-CA in Erp1-depleted embryos induced both the degradation of endogenous Xe-Cdc25A and the T14/Y15 phosphorylation of Cdk1 (Figure 6B); remarkably, it also induced cleavage arrest of the embryos at the two/four-cell stages (Figure 6C). Thus, ERK activation can induce cell cycle arrest at interphase in early embryos.

To test whether the cell cycle arrest by ERK activation was a result of ERK-induced Xe-Cdc25A degradation, we coexpressed MEK-CA and either Xe-Cdc25A WT or its stable 8A mutant in Erp1-depleted embryos. Under the present experimental conditions (see Figure 6B legend), coexpression of Xe-Cdc25A WT did not appreciably affect Cdk1 T14/Y15 phosphorylation or cleavage arrest induced by MEK-CA expression. However, coexpression of the stable 8A mutant greatly reduced the levels of Cdk1 T14/Y15 phosphorylation (Figure 6B) and largely restored embryonic cell divisions (Figure 6C). Thus, clearly, the stable 8A mutant, but not the WT, can overcome ERK-induced cell cycle arrest, indicating that Xe-Cdc25A degradation is responsible for the ERK-induced cell cycle arrest. These results suggest that strong ERK activation can induce cell cycle arrest at interphase by targeting Cdc25A for degradation.

DISCUSSION

Chk1 phosphorylates and targets Cdc25A for $SCF^{\beta\text{-}TrCP}$-dependent degradation both in mammalian cells and *Xenopus* embryos (Busino *et al.*, 2003; Jin *et al.*, 2003; Kanemori *et al.*, 2005). In this study, we have found that the ERK pathway can also phosphorylate and target Xe-Cdc25A for $SCF^{\beta\text{-}TrCP}$-dependent degradation in *Xenopus* eggs. Interestingly, the mechanism of Xe-Cdc25A degradation induced by the ERK pathway is very similar to that induced by Chk1, as summarized in Figure 7.

Our results show that, when strongly activated in *Xenopus* eggs, the ERK–MAPK pathway, but not the JNK or p38 MAPK pathways, can induce prominent phosphorylation and degradation of Xe-Cdc25A (Figure 1, A and B). This

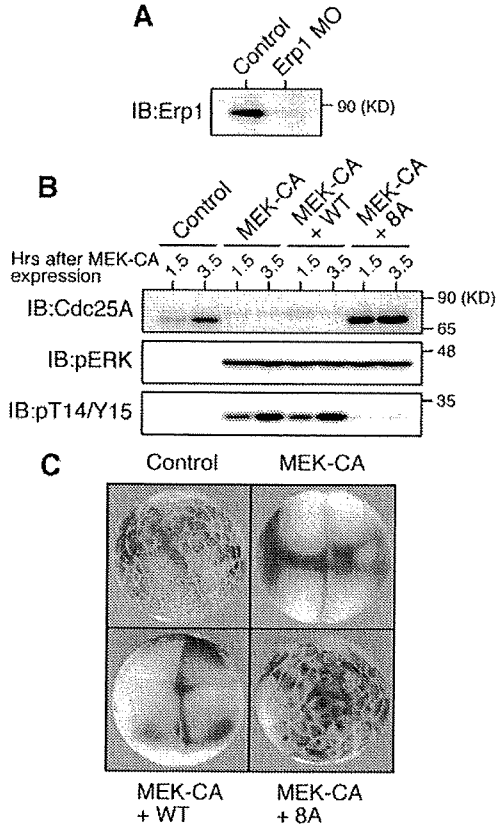

Figure 6. Cell cycle arrest in early embryos by ERK-induced Xe-Cdc25A degradation. (A) One-cell embryos 25 min after fertilization were injected with either water (Control) or 200 ng of Erp1 antisense morpholino oligos (Erp1-MO) and cultured for 1.5 h; embryo extracts were treated with λ-phosphatase and analyzed for endogenous Erp1 by immunoblotting. (B) One-cell embryos injected with Erp1 morpholino oligos as above were cultured for 35 min, injected with either water (Control), 5 ng of MEK-CA mRNA, or both 5 ng of MEK-CA mRNA and 200 pg of Myc-Xe-Cdc25A (WT or 8A) mRNA, cultured for the indicated times, and analyzed for Xe-Cdc25A (endogenous plus exogenous), phospho-ERK, and phospho-T14/Y15 by immunoblotting. (C) The embryos treated as in B were photographed 3 h after injection of MEK-CA mRNA (together with or without Myc-Xe-Cdc25A mRNA). Three and four independent experiments were performed for A and B, respectively, and, for each, a typical result is shown.

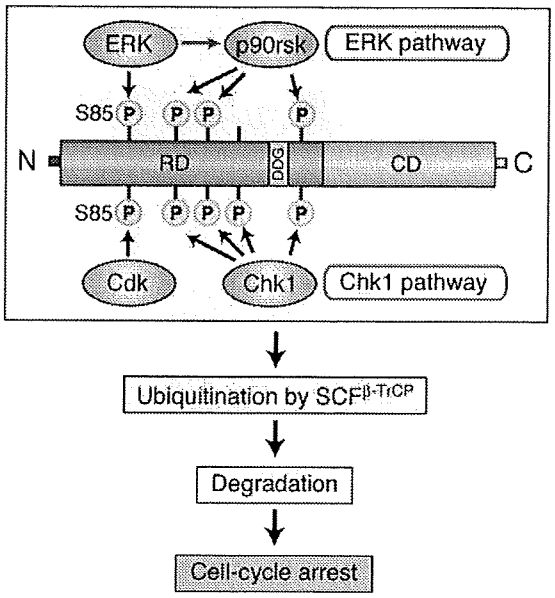

Figure 7. Model for the mechanism of Xe-Cdc25A degradation and cell cycle arrest induced by the ERK pathway. On strong activation of the ERK pathway, ERK phosphorylates Xe-Cdc25A on S85 (which normally is phosphorylated by Cdk) and other Ser residues (omitted), whereas the downstream kinase p90rsk phosphorylates Xe-Cdc25A on other multiple Ser residues (which overlap with Chk1 phosphorylation sites). These phosphorylations facilitate ubiquitination of Xe-Cdc25A by SCF$^{\beta\text{-TrCP}}$, thereby targeting the phosphatase for degradation and causing cell cycle arrest at interphase. For details, see text. RD, regulatory domain; DDG, DDG motif; CD, catalytic domain.

degradation involves the SCF$^{\beta\text{-TrCP}}$ ubiquitin ligase (Figure 1, C and D), similar to Chk1-induced degradation (Kanemori *et al.*, 2005). Furthermore, p90rsk, the kinase downstream of ERK, can phosphorylate Xe-Cdc25A on three of the four Chk1 phosphorylation sites (in the RXXS motifs) (Figure 2B) and thereby can target the phosphatase for degradation, albeit less efficiently than MEK (Figure 2C). Thus, it seems that the ERK pathway can induce Xe-Cdc25A degradation partly because p90rsk phosphorylates Xe-Cdc25A on sites overlapping with Chk1 phosphorylation sites (Figure 7). In this context, it is somewhat surprising that the p38 pathway, which has the Chk1-like kinase MK2 downstream of p38 (Manke *et al.*, 2005) and perhaps thereby targets mammalian Cdc25A for degradation under certain conditions (Khaled *et al.*, 2005; Reinhardt *et al.*, 2007), cannot efficiently induce Xe-Cdc25A degradation in eggs (Figure 1A). This is likely due, at least in part, however, to a relatively low abundance of MK2 protein in *Xenopus* eggs, because overexpression of MK2 (together with the p38 activator MKK6) can induce much more efficient degradation of Xe-Cdc25A in eggs (Supplemental Figure S3). Given our results and the structural analogy between the p38 and the ERK pathways (Raman *et al.*, 2007), MK2 may phosphorylate, at least in part, p90rsk phosphorylation sites, whereas p38 itself may phosphorylate ERK phosphorylation sites (see below), for Xe-Cdc25A degradation.

In addition to p90rsk, ERK itself also phosphorylates Xe-Cdc25A, but, in this case, on several SP motifs (Figure 3, A–D). This phosphorylation, as well as p90rsk phosphorylation (Figure 2A), is required, in part, for MEK-induced Xe-Cdc25A degradation (Figure 4, A and B). Double mutation of the ERK and p90rsk phosphorylation sites, however, renders Xe-Cdc25A (as well as human Cdc25A; Supplemental Figure S2) nearly completely resistant to MEK-induced degradation (Figure 4C). Thus, it seems that ERK phosphorylation and p90rsk phosphorylation contribute, roughly equally and additively, to the MEK-induced degradation of Xe-Cdc25A (as well as of human Cdc25A) (Figure 7). Interestingly, however, S85, the most important ERK phosphorylation site (Figure 4A), is also phosphorylated by Cdk (perhaps Cdk2; Ducruet and Lazo, 2003) in eggs (Figure 3, D and E), although this phosphorylation (by Cdk) is not required for ERK-induced Xe-Cdc25A degradation (because of its phosphorylation by ERK itself) (Figure 3E and Supplemental Figure S1A). Notably, S85 and phosphorylation of its equivalent site S88 are required, in part, for the Chk1-induced degradations of Xe-Cdc25A and human Cdc25A, respectively (Busino *et al.*, 2003; Kanemori *et al.*, 2005), and

Cdk activity is required for Chk1-induced Xe-Cdc25A degradation (our unpublished data). Therefore, S85 of Xe-Cdc25A (as well as S88 of human Cdc25A) is probably phosphorylated by Cdk in the case of Chk1-induced degradation (Figure 7).

How might phosphorylation of the RXXS and SP motifs (by p90rsk and ERK, respectively) act to target Xe-Cdc25A for $SCF^{\beta\text{-}TrCP}$-dependent degradation? This question is important because both the RXXS and SP motifs are located dispersedly far from the DDG motif (to which β-TrCP binds) (Figure 7). Concerning this issue, our preliminary experiments suggested that, whereas the phosphorylation of the RXXS and SP motifs is not necessarily required for β-TrCP binding of Xe-Cdc25A upon ERK activation, it is required significantly for efficient ubiquitination of the phosphatase (data not shown). (This contrasts with the case of human Wee1, in which Cdk phosphorylation of an SP motif near the DDG-like motif promotes both β-TrCP binding and ubiquitination; Watanabe *et al.*, 2005). Thus, it is conceivable that phosphorylation of the RXXS/SP motifs might act to facilitate ubiquitination of Xe-Cdc25A by the bound $SCF^{\beta\text{-}TrCP}$, perhaps by causing conformational changes of the phosphatase (Figure 7). A similar role has been suggested for Chk1-phosphorylated RXXS motifs in both human Cdc25A and Xe-Cdc25A (Busino *et al.*, 2003; Kanemori *et al.*, 2005).

The ERK pathway can target (ectopic) Xe-Cdc25A for $SCF^{\beta\text{-}TrCP}$-dependent degradation even under physiological conditions, or during oocyte maturation, in which the endogenous ERK pathway is fully activated (Figure 5). This result could explain the mechanism for degradation of endogenous Cdc25A during mouse oocyte maturation, which has recently been shown to occur and to be important for meiotic progression of the oocyte (Solc *et al.*, 2008).

Importantly, we find that strong ERK activation can induce cell cycle arrest in early embryos by targeting Xe-Cdc25A for degradation (Figure 6; also see Figure 7). This finding can explain why activating ERK early in cycling egg extracts can cause a G2 arrest (Walter *et al.*, 1997; Bitangcol *et al.*, 1998; Murakami and Vande Woude, 1998). Furthermore, our finding seems to have an important implication in the effects of strongly activated ERK on somatic cells. As is well known, whereas weak or sustained ERK activation is generally mitogenic, strong ERK activation by oncogenic Ras or activated Raf leads to cell cycle arrest in many cell types (and also differentiation in some cases) (Ebisuya *et al.*, 2005; Meloche and Pouyssegur, 2007). This cell cycle arrest may be elicited and maintained primarily by the ERK-induced expression of Cdk inhibitors, such as $p21^{Cip1}$ and $p16^{Ink4a}$ (Pumiglia and Decker, 1997; Serrano *et al.*, 1997; Zhu *et al.*, 1998). Given our results and the degradation of Cdc25A in TPA-treated human cells (Supplemental Figure S4); however, such cell cycle arrest could also be contributed to by an ERK-induced degradation of Cdc25A, similar to cell cycle arrest by Chk1-induced Cdc25A degradation (Donzelli and Draetta, 2003; Bartek and Lukas, 2003). The Ras/Raf- or ERK-induced cell cycle arrest is followed by senescence, a cellular response currently considered to be a defense against neoplasmic transformation (Serrano *et al.*, 1997; Zhu *et al.*, 1998). Thus, degradation of Cdc25A, together with the expression of Cdk inhibitors, might act as a fail-safe mechanism to limit the well-known transforming potential of excessive ERK mitogenic signaling (Lin *et al.*, 1998). In any case, our results suggest that the ERK pathway, when strongly activated, negatively influences cell cycle progression by targeting Cdc25A for $SCF^{\beta\text{-}TrCP}$-dependent degradation.

ACKNOWLEDGMENTS

We thank members of the Sagata laboratory for discussions and K. Gotoh for typing the manuscript. This work was supported by grants from the CREST Research Project of the Japan Science and Technology Agency and from the Ministry of Education, Culture, Sports, Science and Technology of Japan (to N. S.).

REFERENCES

Alonso, G., Ambrosino, C., Jones, M., and Nebreda, A. R. (2000). Differential activation of p38 mitogen-activated protein kinase isoforms depending on signal strength. J. Biol. Chem. *275*, 40641–40648.

Bartek, J., and Lukas, J. (2003). Chk1 and Chk2 kinases in checkpoint control and cancer. Cancer Cell *3*, 421–429.

Bitangcol, J. C., Chau, A.S.S., Stadnick, E., Lohka, M. J., Dicken, B., and Shibuya, E. K. (1998). Activation of the p42 mitogen-activated protein kinase pathway inhibits Cdc2 activation and entry into M-phase in cycling *Xenopus* egg extracts. Mol. Biol. Cell *9*, 451–467.

Busino, L., Donzelli, M., Chiesa, M., Guadavaccaro, D., Ganoth, D., Dorrello, N. V., Hershko, A., Pagano, M., and Draetta, G. F. (2003). Degradation of Cdc25A by β-TrCP during S phase and in response to DNA damage. Nature *426*, 87–91.

Donzelli, M., and Draetta, G. F. (2003). Regulating mammalian checkpoints through Cdc25 inactivation. EMBO Rep. *4*, 671–677.

Ducruet, A. P., and Lazo, J. S. (2003). Regulation of Cdc25A half-life in interphase by cyclin-dependent kinase 2 activity. J. Biol. Chem. *278*, 31838–31842.

Ebisuya, M., Kondoh, K., and Nishida, E. (2005). The duration, magnitude and compartmentalization of ERK MAP kinase activity: mechanisms for providing signaling specificity. J. Cell Sci. *118*, 2997–3002.

Frescas, D., and Pagano, M. (2008). Deregulated proteolysis by the F-box proteins SKP2 and β-TrCP: tipping the scales of cancer. Nat. Rev. Cancer *8*, 438–449.

Frodin, M., and Gammeltoft, S. (1999). Role and regulation of 90 kDa ribosomal S6 kinase (RSK) in signal transduction. Mol. Cell. Endocrinol. *151*, 65–77.

Hoffmann, I., Draetta, G., and Karsenti, E. (1994). Activation of the phosphatase activity of human cdc25A by a cdk2-cyclin E dependent phosphorylation at the G_1/S transition. EMBO J. *13*, 4302–4310.

Inoue, D., Ohe, M., Kanemori, Y., Nobui, T., and Sagata, N. (2007). A direct link of the Mos-MAPK pathway to Erp1/Emi2 in meiotic arrest of *Xenopus laevis* eggs. Nature *446*, 1100–1104.

Jin, J., Shirogane, T., Xu, L., Nalepa, G., Qin, J., Elledge, S. J., and Harper, J. W. (2003). $SCF^{\beta\text{-}TRCP}$ links Chk1 signaling to degradation of the Cdc25A protein phosphatase. Genes Dev. *17*, 3062–3074.

Kanemori, Y., Uto, K., and Sagata, N. (2005). β-TrCP recognizes a previously undescribed nonphosphorylated destruction motif in Cdc25A and Cdc25B phosphatases. Proc. Natl. Acad. Sci. USA *102*, 6279–6284.

Khaled, A. R., Bulavin, D. V., Kittipatarin, C., Li, W. Q., Alvarez, M., Kim, K., Young, H. A., Fornace, A. J., and Durum, S. K. (2005). Cytokine-driven cell cycling is mediated through Cdc25A. J. Cell Biol. *169*, 755–763.

Kim, S.H.Li.C., and Maller, J. L. (1999). A maternal form of the phosphatase Cdc25A regulates early embryonic cell cycles in *Xenopus laevis*. Dev. Biol. *212*, 381–391.

Kishimoto, T. (2003). Cell cycle control during meiotic maturation. Curr. Opin. Cell Biol. *15*, 654–663.

Lei, K., Nimnual, A., Zong, W. X., Kennedy, N. J., Flavell, R. A., Thompson, C. B., Bar-Sagi, D., and Davis, R. J. (2002). The Bax subfamily of Bcl2-related proteins is essential for apoptotic signal transduction by c-Jun NH(2)-terminal kinase. Mol. Cell. Biol. *22*, 4929–4942.

Lin, A. W., Barradas, M., Stone, J. C., van Aelst, L., Serrano, M., and Lowe, S. W. (1998). Premature senescence involving p53 and p16 is activated in response to constitutive MEK/MAPK mitogenic signaling. Genes Dev. *12*, 3008–3019.

Mailand, N., Falck, J., Lukas, C., Syljuåsen, R. G., Welcker, M., Bartek, J., and Lukas, J. (2000). Rapid destruction of human Cdc25A in response to DNA damage. Science *288*, 1425–1429.

Manke, I. A., Nguyen, A., Lim, D., Stewart, M. Q., Elia, A. E., and Yaffe, M. B. (2005). MAPKAP kinase-2 is a cell cycle checkpoint kinase that regulates the G2/M transition and S phase progression in response to UV irradiation. Mol. Cell *17*, 37–48.

Mansour, S. J., Matten, W. T., Hermann, A. S., Candia, J. M., Rong, S., Fukasawa, K., Vande Woude, G. F., and Ahn, N. G. (1994). Transformation of mammalian cells by constitutively active MAP kinase kinase. Science *265*, 966–970.

Meloche, S., and Pouyssegur, J. (2007). The ERK1/2 mitogen-activated protein kinase pathway as a master regulator of the G1- to S-phase transition. Oncogene *26*, 3227–3239.

Molinari, M., Mercurio, C., Dominguez, J., Goubin, F., and Draetta, G. F. (2000). Human Cdc25A inactivation in response to S phase inhibition and its role in preventing premature mitosis. EMBO Rep., *1*, 71–79.

Muda, M., Theodosiou, A., Rodrigues, N., Boschert, U., Camps, M., Gillieron, C., Davies, K., Ashworth, A., and Arkinstall, S. (1996). The dual specificity phosphatases M3/6 and MKP-3 are highly selective for inactivation of distinct mitogen-activated protein kinases. J. Biol. Chem. *271*, 27205–27208.

Murakami, M. S., and Vande Woude, G. F. (1998). Analysis of the early embryonic cell cycles of *Xenopus*; regulation of cell cycle length by Xe-wee1 and Mos. Development *125*, 237–248.

Nishiyama, T., Ohsumi, K., and Kishimoto, T. (2007). Phosphorylation of Erp1 by p90rsk is required for cytostatic factor arrest in *Xenopus laevis* eggs. Nature, *446*, 1096–1099.

Okamoto, K., and Sagata, N. (2007). Mechanism for inactivation of the mitotic inhibitory kinase Wee1 at M phase. Proc. Natl. Acad. Sci. USA *104*, 3753–3758.

Pumiglia, K. M., and Decker, S. J. (1997). Cell cycle arrest mediated by the MEK/mitogen-activated protein kinase pathway. Proc. Natl. Acad. Sci. USA *94*, 448–452.

Raman, M., Chen, W., and Cobb, M. H. (2007). Differential regulation and properties of MAPKs. Oncogene *26*, 3100–3112.

Reinhardt, H. C., Aslanian, A. S., Lees, J. A., and Yaffe, M. B. (2007). p53-deficient cells rely on ATM- and ATR-mediated checkpoint signaling through the p38MAPK/MK2 pathway for survival after DNA damage. Cancer Cell *11*, 175–189.

Sagata, N. (1997). What does Mos do in oocytes and somatic cells? Bioessays *19*, 13–21.

Serrano, M., Lin, A. W., McCurrach, M. E., Beach, D., and Lowe, S. W. (1997). Oncogenic *ras* provokes premature cell senescence associated with accumulation of p53 and p16INK4a. Cell *88*, 593–602.

Shimuta, K., Nakajo, N., Uto, K., Hayano, Y., Okazaki, K., and Sagata, N. (2002). Chk1 is activated transiently and targets Cdc25A for degradation at the *Xenopus* midblastula transition. EMBO J. *21*, 3694–3703.

Solc, P., Saskova, A., Baran, V., Kubelka, M., Schultz, R. M., and Motlik, J. (2008). CDC25A phosphatase controls meiosis I progression in mouse oocytes. Dev. Biol. *317*, 260–269.

Sturgill, T. M., Ray, L. B., Erikson, E., and Maller, J. L. (1988). Insulin-stimulated MAP-2 kinase phosphorylates and activates ribosomal protein S6 kinase II. Nature *334*, 715–718.

Uto, K., Inoue, D., Shimuta, K., Nakajo, N., and Sagata, N. (2004). Chk1, but not Chk2, inhibits Cdc25 phosphatases by a novel common mechanism. EMBO J. *23*, 3386–3396.

Walter, S. A., Guadagno, T. M., and Ferrell,, J. E., Jr. (1997). Induction of a G_2-phase arrest in *Xenopus* egg extracts by activation of p42 mitogen-activated protein kinase. Mol. Biol. Cell. *8*, 2157–2169.

Yamanaka, H., Moriguchi, T., Masuyama, N., Kusakabe, M., Hanafusa, H., Takeda, R., Takeda, S., and Nishida, E. (2002). JNK functions in the non-canonical Wnt pathway to regulate convergent extension movements in vertebrates. EMBO Rep. *3*, 69–75.

Watanabe, N., Arai, H., Iwasaki, J. -I., Shiina, M., Ogata, K., Hunter, T., and Osada, H. (2005). Cyclin-dependent kinase (CDK) phosphorylation destabilizes somatic Wee1 via multiple pathways. Proc. Natl. Acad. Sci. USA *102*, 11663–11668.

Zhu, J., Woods, D., McMahon, M., and Bishop, J. M. (1998). Senescence of human fibroblasts induced by oncogenic Raf. Genes Dev. *12*, 2997–3007.

J Neurooncol
DOI 10.1007/s11060-010-0147-3

LABORATORY INVESTIGATION - HUMAN/ANIMAL TISSUE

CDC25A mRNA levels significantly correlate with Ki-67 expression in human glioma samples

Yoji Yamashita · Isao Kasugai · Masami Sato · Nobuhiro Tanuma · Ikuro Sato · Miyuki Nomura · Katsumi Yamashita · Yukihiko Sonoda · Toshihiro Kumabe · Teiji Tominaga · Ryuichi Katakura · Hiroshi Shima

Received: 4 December 2009 / Accepted: 15 February 2010

Abstract Cell division cycle 25 (CDC25) phosphatases are cell-cycle regulatory proteins which are overexpressed in a significant number of human cancers. This study evaluated the role of CDC25 phosphatases in human glioma proliferation. Upregulation of CDC25A was observed in human glioma specimens and human glioma cell lines. Comparison of expression levels of CDC25A and CDC25B messenger ribonucleic acid (RNA) to Ki-67 labeling index in glioma tissues found that Ki-67 labeling index was significantly correlated with the expression of CDC25A, but not with that of CDC25B. Depletion of CDC25A by small interfering RNA and inhibition of CDC25 suppressed cell proliferation and induced apoptosis in glioma cell lines, indicating that CDC25A is a potential target for the development of new therapy for glioma.

Keywords CDC25A · Glioma · Ki-67 · Protein phosphatase

Yoji Yamashita and Isao Kasugai contributed equally to this work.

Y. Yamashita · I. Kasugai · M. Sato · N. Tanuma · M. Nomura · H. Shima (✉)
Division of Cancer Chemotherapy, Miyagi Cancer Center Research Institute, 47-1 Nodayama, Medeshima-Shiode, Natori, Miyagi 981-1293, Japan
e-mail: shima-hi632@pref.miyagi.jp

Y. Yamashita · R. Katakura
Department of Neurosurgery, Miyagi Cancer Center, Natori, Miyagi, Japan

I. Sato
Section of Clinical Research, Miyagi Cancer Center Research Institute, Natori, Miyagi, Japan

K. Yamashita
Division of Life Science, Graduate School of Natural Science and Technology, Kanazawa University, Kanazawa, Ishikawa, Japan

Y. Sonoda · T. Kumabe · T. Tominaga
Department of Neurosurgery, Tohoku University Graduate School of Medicine, Sendai, Miyagi, Japan

Introduction

Glioblastomas are the most common and lethal type of malignant brain tumor. Median survival from the time of diagnosis is less than a year, with fewer than 5% of patients surviving 5 years. Glioblastoma is characterized by highly proliferative and invasive activity, and widespread infiltration of tumor cells into the surrounding brain tissue [1]. Recent standard therapy for glioblastomas includes surgical resection, radiotherapy, and adjuvant temozolomide chemotherapy administered both during and after radiotherapy. However, most patients develop tumor recurrence or progression after this multimodality treatment. There is clearly an urgent need to develop new classes of treatment modalities, such as molecular target-directed therapies [2–4]. Understanding the molecular pathogenesis of glioma may allow the rational development of new therapy approaches.

The rate of cell proliferation in glioma tissues as assessed by Ki-67 immunoreactivity has been studied as a prognostic indicator, and correlates with tumor grade and clinical course [5, 6]. Ki-67 detected by MIB-1 antibody is a core antigen present in proliferating cells and absent in quiescent cells. This antigen is expressed in all phases of the cell cycle except for G0 and the early parts of G1. The precise function of the Ki-67 protein is still unclear. Therefore, identification of molecules involved in the upregulation of Ki-67 antigen may help to understand the

Published online: 10 March 2010

malignant phenotype of glioma, and may become a candidate target for treatment.

Regular control of cell cycle progression requires correct function of a small family of phosphatases termed cell division cycle 25 (CDC25), which contain highly conserved domains for dual specificity phosphatases [7]. The CDC25 family is fundamental in transitions between cell cycle phases during normal cell division through the activation of cyclin-dependent kinase (CDK)/cyclin complexes. Three genes code for the CDC25A, B, and C proteins with both different and redundant specificities and regulations in humans. In particular, the CDC25A and B phosphatases have oncogenic properties and are overexpressed singly in some types of cancers and together in others [8]. Therefore, CDC25s are promising targets for the development of new anticancer therapeutic strategies. Overexpression of CDC25 is linked to clinicopathological features such as tumor grade, recurrent disease, or disease-free survival [9, 10].

The present study examined whether CDC25 isotype-specific linkage is present in human glioblastoma samples.

Materials and methods

Patients and glioma samples

Newly diagnosed human glioma tissues were obtained from 25 consecutive patients (15 males and 10 females) who underwent surgery (14 surgical resections and 11 stereotactic biopsies) at the Department of Neurosurgery, Miyagi Cancer Center, from July 2008 onwards. Their median age was 63 years (range 21–83). Without regard to tumor volumes or tumor malignancies, small samples weighing from 10 to 30 mg were collected for this study from all surgical specimens and serial numbers were added in the order of surgery. Each sample was immediately divided in two. One was frozen for ribonucleic acid (RNA) preparation, the other was formalin-fixed and paraffin-embedded for conventional histopathological evaluation and counting of Ki-67 labeling index (Ki-67LI). Histological diagnoses were made by a neuropathologist, based on the World Health Organization criteria as glioblastoma (16 cases; nos. 1–5, 7–12, 14, 18–21), anaplastic astrocytoma (6 cases; nos. 6, 13, 17, 23–25), and diffuse astrocytoma (3 cases; nos. 15, 16, 22). RNA analysis was approved by the Ethics Committee of the Miyagi Cancer Center.

Quantitative real-time polymerase chain reaction

Total RNA was prepared from the specimens with the RNeasy Lipid Mini kit (Qiagen). Complementary deoxyribonucleic acid (cDNA) was synthesized using an oligo-d(T)12-18 primer with Superscript III reverse transcriptase (Invitrogen) and applied to quantitative real-time polymerase chain reaction (qPCR) using the LightCycler 480 and the probes master kit (Roche Diagnostics). The PCR primers and the probes were designed and selected for the intron spanning condition according to the online software (Roche Applied Science). The PCR reaction was performed in 20 μl containing 10 μl of Probes Master (Roche), 0.5 μM of each primer, 0.1 μM of probe, and 5 μl of cDNA solution. The protocol of PCR involved initial denaturation at 95°C for 5 min, followed by 55 cycles of 95°C for 10 s, then 60°C for 25 s. Threshold cycle values (Second Derivative Maximum method) were normalized to the housekeeping gene, porphobilinogen deaminase (PBGD). Human brain (frontal lobe) total RNA from a pool of four different donors and from single donor were obtained from Clontech (Palo Alto, CA, USA) and BioChain Institute (Hayward, CA), respectively, were also subjected to cDNA synthesis and subsequent qPCR. The levels of CDC25A and CDC25B messenger RNA (mRNA) in the gliomas were expressed as ratios to that of the mixed human brain RNA sample (Clontech). The following probes were used: no. 17 (CDC25A), no. 68 (CDC25B), no. 2 (CDC25C), and no. 25 (PBGD) (Roche Universal Probe Library). The primer sequences were as follows: CDC25A 5′-TCTGAAGAATGAGGAGGAGACC-3′ and 5′-AAACAGCTTGCATCGGTTGT-3′; CDC25B 5′-ACG CCCGTGCAGAATAAG-3′ and 5′-AGTGATTTTGAG CGGAGGAC-3′; CDC25C 5′-GAGGCCATGTCGGAA GAAG-3′ and 5′-GCTTCCTTCCTCTCTTGTGG-3′; PBGD 5′-AGCTATGAAGGATGGGCAAC-3′ and 5′-TTGTATG CTATCTGAGCCGTCTA-3′.

Ki-67LI

Ki-67LI was measured. Fields with the highest number of Ki-67-labeled cells were initially selected through generalized survey, and then the percentage of positive-labeled cells was determined by counting more than 1,000 tumor nuclei of more than three fields of a specimen at ×400 magnification without knowing any clinical information. Only strong nuclear staining was regarded as positive, and weak nuclear or cytoplasmic staining was regarded as negative.

Statistical analysis

Statistical analysis used the software Statview 5.0 (SAS Institute, Cary, NC). The expression level of CDC25A mRNA was compared with the Ki-67LI in human primary glioblastoma samples using simple linear regression analysis, and a P value of less than 0.05 was considered to indicate statistical significance.

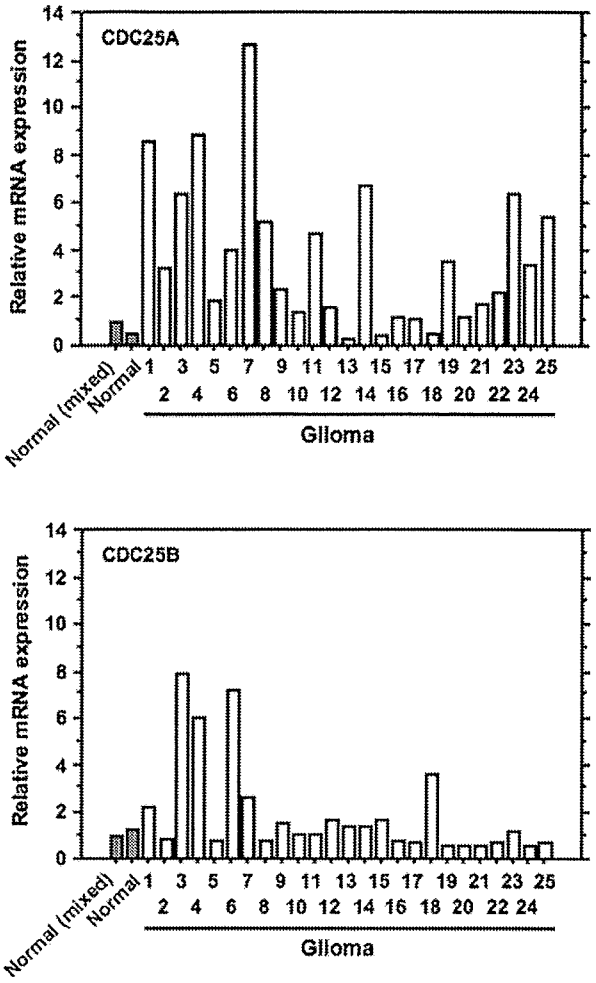

Fig. 1 Analysis of *CDC25A* and *CDC25B* mRNA levels in human glioma samples. Expression levels of *CDC25A* (*upper*) or *CDC25B* (*lower*) mRNA in normal brain and primary glioblastoma samples were estimated by qPCR. Results were normalized to the mRNA levels of the housekeeping gene porphobilinogen deaminase (PBGD) and shown relative to mRNA levels seen in the normal brain (four mixed samples), which was set as 1.0

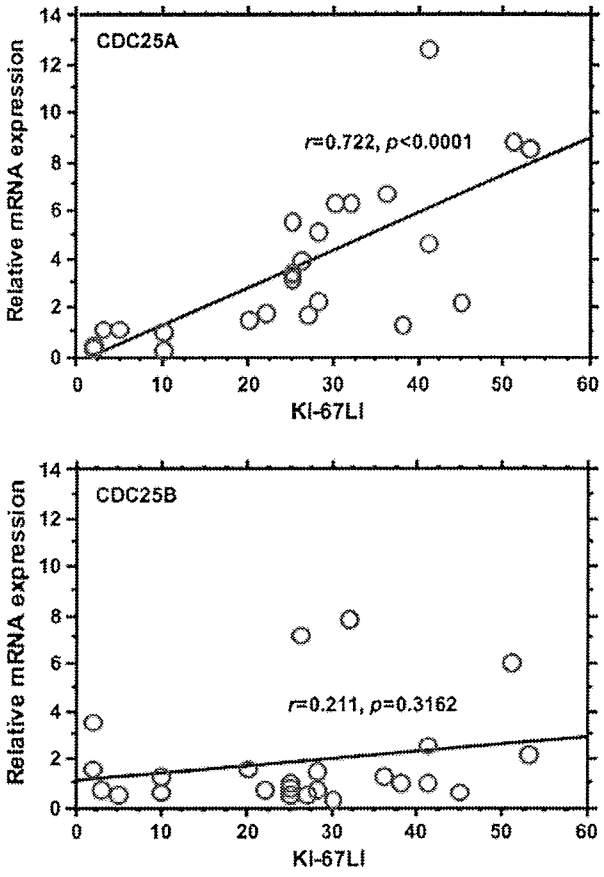

Fig. 2 Statistical comparison of the expression levels of *CDC25A* and *CDC25B* mRNA with *Ki-67LI* in human primary glioma samples. Simple linear regression analysis showed the relationship between the expression of *CDC25A* (*upper*) or *CDC25B* (*lower*) mRNA and *Ki-67LI* in human primary glioblastoma samples

Cell culture

Human glioblastoma cell line A172 was obtained from the RIKEN BRC (Tsukuba, Ibaraki, Japan), and U87, U251, and U373 were obtained from DS PHARMA Biomedical (Osaka, Japan), Health Science Research Resources Bank (Osaka, Japan), and ATCC, respectively. A172, U87, U251, and U373 cells were maintained in Dulbecco's modified Eagle's medium supplemented with 10% fetal bovine serum (FBS). A172 cells were cultured in RPMI-1640 (Gibco) supplemented with 10% FBS. Normal human astrocytes (NHAs) (Lonza, Basel, Switzerland) were cultured in Astrocyte Basal Medium supplemented with AGM SingleQuots according to the manufacturer's instructions. NHA proliferation was arrested after 21 days culture, and used as quiescent cells.

Small interfering RNA transfection

Small interfering RNA (siRNA) duplexes against human CDC25A (Stealth RNAi), HSS101654 (siRNA1-CDC25A), and HSS10165 (siRNA2-CDC25A) were purchased from Invitrogen. Stealth RNAi Negative Control Medium GC duplex (Invitrogen) was used as the control. siRNA transfection was undertaken using Lipofectamine RNAiMAX (Invitrogen) according to the manufacturer's instruction at a final siRNA concentration of 5 nM in the culture.

Cell proliferation assay

Cells transfected with siRNA or small compounds were plated on a 96-well plate in octuplicate wells. Cell

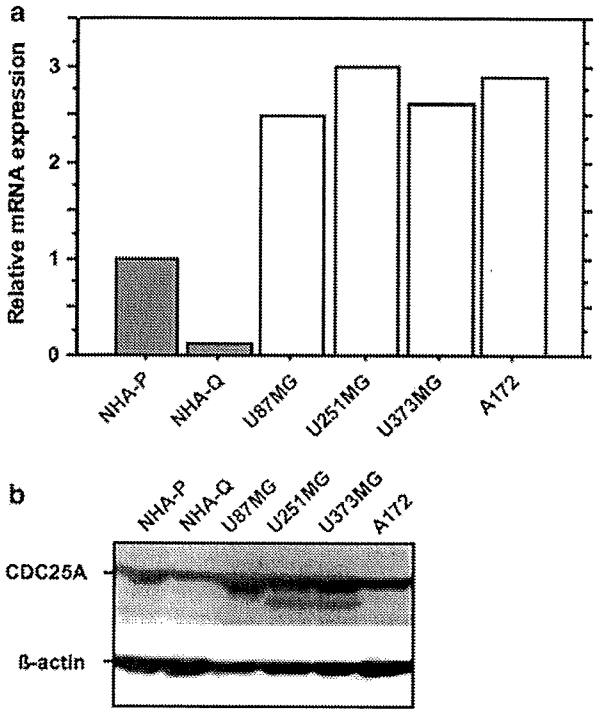

Fig. 3 Analyses of CDC25A mRNA levels (**a**) and protein levels (**b**) in human glioma cell lines. **a** Expression levels of CDC25A mRNA in normal human astrocytes in the proliferating (*NHA-P*) and quiescent stages (*NHA-Q*) and glioma cell line samples were estimated by qPCR. Results were normalized to the mRNA levels of the housekeeping gene porphobilinogen deaminase (PBGD) and shown relative to the mRNA levels seen in normal brain (four mixed samples), which was set as 1.0. **b** Immunoblot analysis of *CDC25A* in normal human astrocytes and glioma cell lines

proliferation was assessed as incorporation of 1-methoxy PMS by the DOJINDO cell counting Kit-8 according to the manufacture's protocol (DOJINDO, Kumamoto, Japan). Optical density was read at 450 nm at various time points using a microplate reader (TECAN, Research Triangle Park). The corresponding background value was subtracted from the reading obtained from each well. To estimate half maximal inhibitory concentration (IC50) for each compound, values at 96 h of treatment were used for linear regression analysis.

Caspase-3 and -7 activity

To measure apoptosis in glioma cell lines treated with siRNAs or small compounds, the cells were plated on a 96-well plate in triplicate wells. The caspase-3 and -7 enzyme activities were measured by the Caspase-Glo 3/7 Assay (Promega) according to the manufacturer's protocol.

Results

Upregulation of CDC25A in human glioma samples

The expression level of the three CDC25 family members (CDC25A, B, and C) was examined in 25 human glioma samples by qPCR. Figure 1 shows the mRNA levels of CDC25A and CDC25B in the glioma samples compared to that in normal (mixed) brain. The CDC25A and CDC25B mRNAs were elevated in 17 (68%) and 6 (24%), respectively, of these samples. In contrast, the CDC25C mRNA level was under the detection limit in the normal brain, and no induction was observed in tumor samples.

Correlation of CDC25A expression with Ki-67LI

To examine the possible involvement of CDC25A and CDC25B in cellular proliferation, the expression of Ki-67, a marker for cell proliferation, was examined by immunohistochemistry with MIB-1 antibody. Figure 2 shows that Ki-67LI levels were significantly correlated with the level of CDC25A ($r = 0.722$, $P < 0.0001$), but not with that of CDC25B ($r = 0.211$, $P = 0.3162$). Therefore, overexpression of CDC25A rather than CDC25B is involved in increased cell proliferation in glioma tissues.

Upregulation of CDC25A in human glioma cell lines

CDC25A expression was examined in 4 glioma cell lines, U87MG, U251MG, U373MG, and A172. NHAs in the proliferating and quiescent stages were used as controls. Figure 3a shows the relative expression of CDC25A in these cells. The level of CDC25A mRNA was reduced to 20% after the end of proliferation in NHAs, supporting the importance of CDC25A expression in cell proliferation. Compared to proliferating NHAs, glioma cell lines such as U87MG, U251MG, U373MG, and A172 showed 2- to 3-fold increase in CDC25A mRNA expression. Analysis of the CDC25A protein levels in these cells showed almost similar levels to those of CDC25A mRNA (Fig. 3b). Therefore, CDC25A is overexpressed in glioma cell lines.

Inhibitor of CDC25 suppresses cell proliferation

To examine the role of CDC25s in glioblastoma, the effects of two quinone-based CDC25 inhibitors, BN82002 [11] and BN82685 [12], were analyzed on cell proliferation in U87MG and A172 cells (Fig. 4a). Both compounds inhibited CDC25A and CDC25B, and they were already reported to be active not only in vitro but also in vivo [11, 12]. U87MG and A172 cells were treated with increasing concentrations of the inhibitors until 96 h. The IC50s of

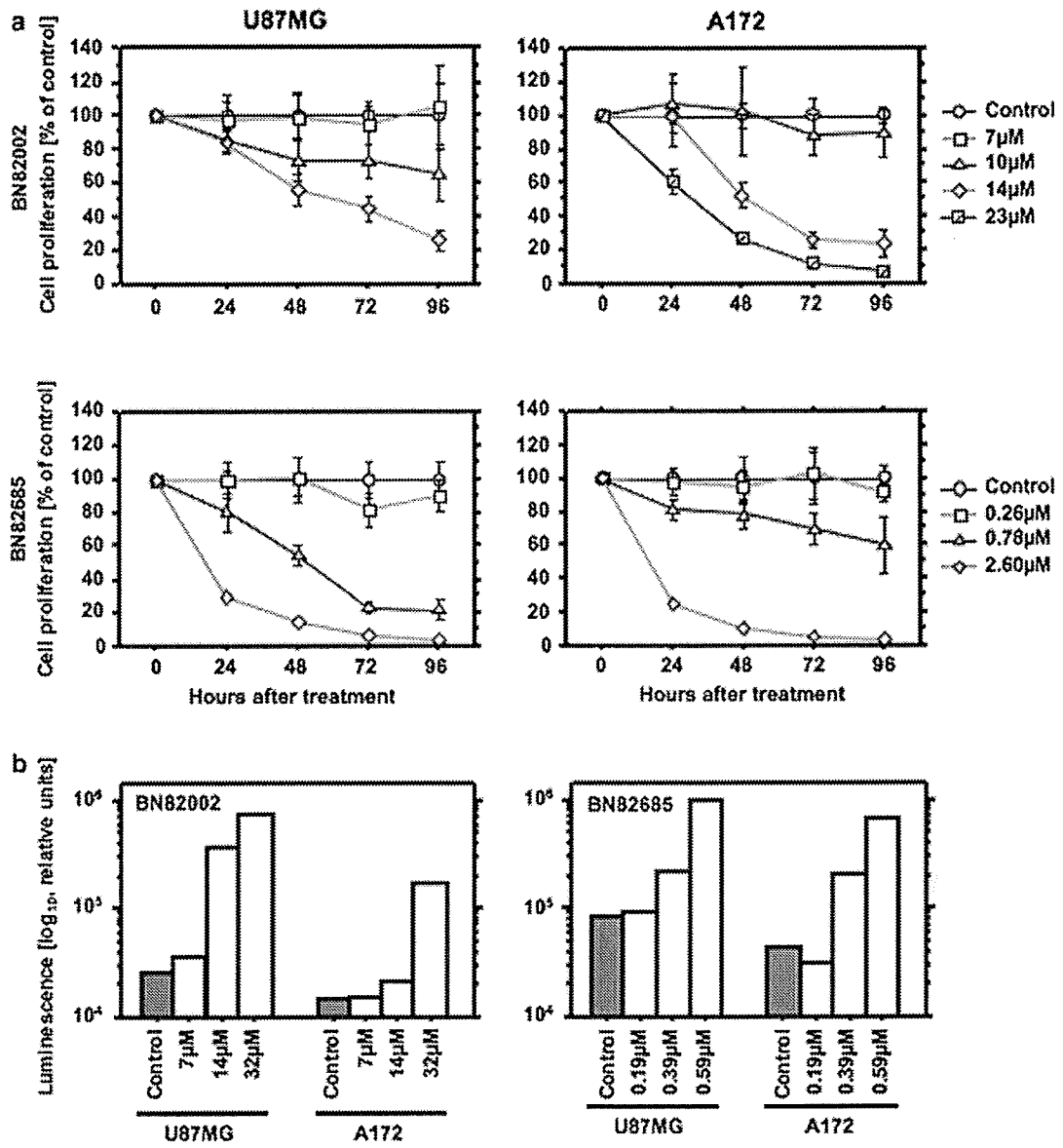

Fig. 4 Inhibition of CDC25 reduces cell proliferation (**a**) and induces cell apoptosis (**b**). *U87MG* and *A172* cells were grown in 98-well plates and treated with dimethyl sulfoxide (*control*) or CDC25 inhibitors, *BN82002* or *BN82685*. Cell proliferation assay (**a**) and caspase-3 and -7 assay (**b**) as described in "Materials and methods"

BN82002 for U87MG and A172 were 18 and 12 μM, respectively, and the IC50s of BN82685 for U87MG and A172 were 0.54 and 0.90 μM, respectively. In addition, BN82002 and BN82685 dose-dependently induced apoptosis, as assessed by the caspase-3 and -7 activities (Fig. 4b).

Silencing of CDC25A inhibits cell growth

To evaluate the CDC25A specific role in proliferation and survival in glioma cells, the siRNA approach was used to deplete CDC25A in the glioma cell lines. Two CDC25A-specific siRNA (siRNA1-CDC25A and siRNA2-CDC25A) and negative control siRNA were transfected into U87MG and A172 cells, both of which overexpressed CDC25A. Immunoblot analysis confirmed suppression of CDC25A expression in siRNA1-CDC25A and siRNA2-CDC25A at days 2 and 3 after transfection (Fig. 5a).

The effects of CDC25A suppression on the cell proliferation of the glioma cells were analyzed. U87MG and A172 were transfected with siRNA1-CDC25A, siRNA2-CDC25A, or control siRNA, and cell proliferation was assessed daily over 5 days (Fig. 5b). Both cell lines

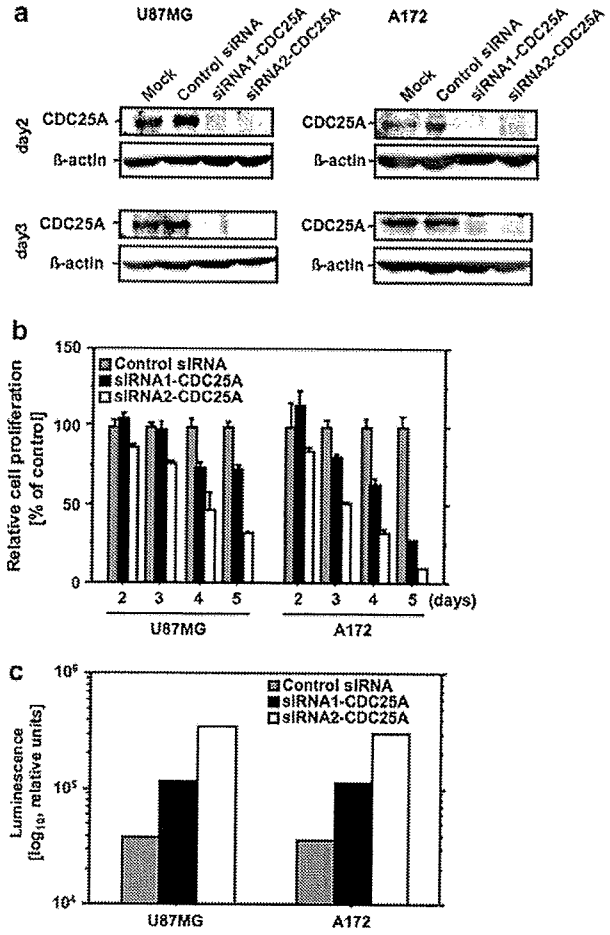

Fig. 5 Suppression of CDC25A by siRNA treatment inhibits cell proliferation and induces apoptosis in glioma cells. *U87MG* and *A172* cells were transfected with control siRNA or siRNAs against human CDC25A as described in "Materials and methods" and cultured for the indicated times. The cells were lysed and immunoblot was performed using antibody for CDC25A or β-actin (**a**). Cell proliferation assay (**b**) and caspase-3 and -7 assay (**c**) as described in "Materials and methods"

transfected with siRNA1-CDC25A and siRNA2-CDC25A showed slower growth rates than cells transfected with control siRNA. Additionally, caspase activity was measured in the CDC25A-depleted cells. The U87MG and A172 cells transfected with the CDC25A siRNAs showed increased levels of caspase, demonstrating that apoptosis was induced in the CDC25A-depleted cells (Fig. 5c). Therefore, CDC25A-mediated cell proliferation and survival in glioma cells, and suppression resulted in growth inhibition.

Discussion

The present study investigated expression levels of CDC25s in human gliomas, and found that CDC25A is overexpressed, and that its expression level is closely correlated with Ki-67LI in gliomas. This may be the first functional molecule with expression well correlated with Ki-67LI in glioma tissues.

CDC25 was overexpressed and contributed to tumorigenesis in various patients with high-grade malignant tumor [8]. Both CDC25 A and B have prognostic value. Overexpression of CDC25B and significant correlation of expression with shorter periods of disease-free survival were found in glioma samples, but the level of CDC25A expression was not defined [13]. CDC25 overexpression within each cancer subtype tends to occur in an isoform-specific manner, and the overexpression of multiple isoforms in the same cancer subtypes probably occurs through independent pathways [8].

This study showed that expression of CDC25A was more prominent and correlated better with Ki-67LI than expression of CDC25B in glioma tissues. These findings indicate that overexpression of CDC25A rather than CDC25B is involved in increased cell proliferation in glioma tissues. The majority of studies have clearly shown the prognostic importance of Ki-67LI in glioma, both regarding survival and recurrence [5, 6], so CDC25A should be considered the marker for prognosis and/or target for treatment rather than CDC25B.

The present study showed overexpression of CDC25A in both surgical specimens and glioma cell lines. CDC25A expression was 2–3 times higher in glioma cell lines than the proliferating NHAs, suggesting overexpression of CDC25A characterizes the malignant phenotype of glioma cells. The mechanisms by which CDC25 isoforms become deregulated during tumorigenesis remains unclear. Several positive and/or negative regulators of CDC25A transcription have been described, including c-myc, hypoxia-inducible factor-1 alpha, p53, p21, and E2F, but there is no evidence that CDC25 overexpression resulted from gene amplification or rearrangements, or any other specific genetic mutations that may be responsible for deregulating CDC25 activities in cancer [8]. The development of CDC25A targeting therapy will require further studies to reveal the CDC25 biology in glioma.

Recently, CDKs are crucial in the control of the cell cycle, so are attractive pharmacological targets for the development of antiproliferative agents. Inhibitors of these enzymes are currently in clinical trials in patients with various malignant tumors. CDC25s are activators of CDKs, so are particularly attractive target candidates for the development of anticancer agents. Various classes of CDC25 inhibitors have been identified, and the specificities were examined in vitro. We selected BN82002 and BN82685 because of their relatively higher selectivity for CDC25A. The IC50s of BN82002 towards CDC25A, CDC25B2, and CDC25B3 are 2.4, 3.9, and 6.3 μM, and

those of BN82685 are 109, 160, and 249 nM, respectively, in vitro [11, 12]. In this study, these inhibitors showed remarkable growth suppression and induction of apoptosis in glioma cells, and similar effects were observed after selective depletion of CDC25A from glioma cells by siRNA. These results suggest that CDC25A is important in glioma cell proliferation and survival, and CDC25A targeted therapy using isoform specific inhibitor is a potential approach to glioma therapy.

Acknowledgments This work was supported in part by Grants-in-aid for Scientific Research (C) to Y.Y. and H.S. and for Exploratory Research to R.K. provided by the Japan Society for the Promotion of Science.

References

1. Ohgaki H, Kleihues P (2007) Genetic pathways to primary and secondary glioblastoma. Am J Pathol 170:1445–1453
2. Sathornssumetee S, Reardon DA, Desjardins A, Quinn JA, Vredenburgh JJ, Rich JN (2007) Molecularly targeted therapy for malignant glioma. Cancer 110:13–24
3. Parsons DW, Jones S, Zhang X, Lin JC, Leary RJ, Angenendt P, Mankoo P, Carter H, Siu IM, Gallia GL, Olivi A, McLendon R, Rasheed BA, Keir S, Nikolskaya T, Nikolsky Y, Busam DA, Tekleab H, Diaz LA Jr, Hartigan J, Smith DR, Strausberg RL, Marie SK, Shinjo SM, Yan H, Riggins GJ, Bigner DD, Karchin R, Papadopoulos N, Parmigiani G, Vogelstein B, Velculescu VE, Kinzler KW (2008) An integrated genomic analysis of human glioblastoma multiforme. Science 321:1807–1812
4. Rich JN, Hans C, Jones B, Iversen ES, McLendon RE, Rasheed BK, Dobra A, Dressman HK, Bigner DD, Nevins JR, West M (2005) Gene expression profiling and genetic markers in glioblastoma survival. Cancer Res 65:4051–4058
5. Faria MH, Gonçalves BP, do Patrocínio RM, de Moraes-Filho MO, Rabenhorst SH (2006) Expression of Ki-67, topoisomerase IIalpha and c-MYC in astrocytic tumors: correlation with the histopathological grade and proliferative status. Neuropathology 26:519–527
6. Johannessen AL, Torp SH (2006) The clinical value of Ki-67/MIB-1 labeling index in human astrocytomas. Pathol Oncol Res 12:143–147
7. Boutros R, Dozier C, Ducommun B (2006) The when and wheres of CDC25 phosphatases. Curr Opin Cell Biol 18:185–191
8. Boutros R, Lobjois V, Ducommun B (2007) CDC25 phosphatases in cancer cells: key players? Good targets? Nat Rev Cancer 7:495–507
9. Kiyokawa H, Ray D (2008) In vivo roles of CDC25 phosphatases: biological insight into the anti-cancer therapeutic targets. Anticancer Agents Med Chem 8:826–832
10. Lazo JS, Wipf P (2008) Is Cdc25 a druggable target? Anticancer Agents Med Chem 8:837–842
11. Brezak MC, Quaranta M, Mondésert O, Galcera MO, Lavergne O, Alby F, Cazales M, Baldin V, Thurieau C, Harnett J, Lanco C, Kasprzyk PG, Prevost GP, Ducommun B (2004) A novel synthetic inhibitor of CDC25 phosphatases: BN82002. Cancer Res 64:3320–3325
12. Brezak MC, Quaranta M, Contour-Galcera MO, Lavergne O, Mondesert O, Auvray P, Kasprzyk PG, Prevost GP, Ducommun B (2005) Inhibition of human tumor cell growth in vivo by an orally bioavailable inhibitor of CDC25 phosphatases. Mol Cancer Ther 4:1378–1387
13. Nakabayashi H, Hara M, Shimizu K (2006) Prognostic significance of CDC25B expression in gliomas. J Clin Pathol 59:725–728

Biochemical and Biophysical Research Communications 390 (2009) 636–641

Contents lists available at ScienceDirect

Biochemical and Biophysical Research Communications

journal homepage: www.elsevier.com/locate/ybbrc

An animal model of preclinical diagnosis of pancreatic ductal adenocarcinomas

Katsumi Fukamachi [a], Hajime Tanaka [b], Yoshiaki Hagiwara [d,e], Hirotaka Ohara [b], Takashi Joh [b], Masaaki Iigo [a], David B. Alexander [a], Jiegou Xu [a], Ne Long [a], Misato Takigahira [f,g], Kazuyoshi Yanagihara [f,h], Okio Hino [e], Izumu Saito [i], Hiroyuki Tsuda [a,c,*]

[a] Department of Molecular Toxicology, Nagoya City University Graduate School of Medical Sciences, 1 Kawasumi, Mizuho-cho, Mizuho-ku, Nagoya 467-8601, Japan
[b] Department of Gastroenterology and Metabolism, Nagoya City University Graduate School of Medical Sciences, 1 Kawasumi, Mizuho-cho, Mizuho-ku, Nagoya 467-8601, Japan
[c] Nanotoxicology Project, Nagoya City University Graduate School of Medical Sciences, 1 Kawasumi, Mizuho-cho, Mizuho-ku, Nagoya 467-8601, Japan
[d] Immuno-Biological Laboratories, 5-1 Aramachi, Takasaki-Shi, Gunma 370-0831, Japan
[e] Department of Pathology and Oncology, Juntendo University School of Medicine, 2-1-1 Hongo, Tokyo 113-8421, Japan
[f] Central Animal Laboratory, National Cancer Center Research Institute, 5-1-1 Tsukiji, Chuo-ku, Tokyo 104-0045, Japan
[g] Gastrointestinal Section, National Cancer Center Hospital, 5-1-1 Tsukiji, Chuo-ku, Tokyo 104-0045, Japan
[h] Laboratory of Health Sciences, Department of Life Sciences, Yasuda Women's University, 6-13-1 Yasuhigashi, Asaminami-ku, Hiroshima 731-0153, Japan
[i] Laboratory of Molecular Genetics, Institute of Medical Science, University of Tokyo, 4-6-1 Shirokanedai, Minato-ku, Tokyo 108-8639, Japan

ARTICLE INFO

Article history:
Received 3 October 2009
Available online 8 October 2009

Keywords:
Pancreas cancer
Serum marker
Erc
Mesothelin
Animal model

ABSTRACT

Pancreatic ductal adenocarcinoma (PDA) is a highly lethal disease, which is usually diagnosed in an advanced stage. Animal PDA models which reflect the human condition are clearly necessary to develop early diagnostic tools and explore new therapeutic approaches. We have established transgenic rats carrying a mutated H- or K-*ras* gene (Hras250 and Kras327) controlled by Cre/loxP activation. These animals develop PDA which are histopathologically similar to that in humans. We utilized this model to identify biomarkers to detect early PDA. We report here that serum levels of Erc/Mesothelin are significantly higher in rats bearing PDA than in controls. Importantly, the levels are significantly elevated in rats before grossly visible carcinomas develop. Even in rats with very small microscopic ductal carcinoma lesions, elevated serum Erc/Mesothelin can be detected. We believe this is the first report of a pancreas tumor animal model in which pre-symptomatic lesions can be diagnosed.

Introduction

Pancreatic ductal adenocarcinoma (PDA) carries the most dismal prognosis of all solid tumors. Preclinical detection of PDA is a necessary first step toward more successful treatment of this disease. Late manifestation of clinical symptoms, as well as the rapid and aggressive course of the disease contribute to its extremely high mortality. Most patients die within 1 year of diagnosis [1], and the 5 year survival rate is <5% [2]. Since the pancreas is located in a retroperitoneal cavity, detection of the tumor mass is possible only when it has reached a relatively large size. Furthermore, markers for the diagnosis of PDA have not yet been established. Consequently, diagnosis of pancreatic cancers when they are still treatable is extremely rare [3].

We have established transgenic rat lines carrying a human $Hras^{G12V}$ (Hras250) [4] or a human $Kras^{G12V}$ (Kras327) oncogene in which the expression of the transgene is regulated by the Cre/loxP system (termed *ras* Tg rats). Targeted activation of the transgene is accomplished by injection of a Cre recombinase-carrying adenovirus (AxCANCre) into the pancreatic ducts through the common bile duct. Neoplastic lesions in the *ras* Tg rats exhibit morphological similarities to those observed in human pancreas lesions. Early ductal lesions exhibit close similarity to intraepithelial neoplasias (PanIN category).

The rat *Erc* (expressed in renal cell carcinoma) gene was identified as a highly expressed gene in renal cell carcinoma of the Eker rat [5,6]. A human homolog of rat *Erc* is the *Mesothelin/megakaryocyte potentiating factor* (*MPF*) gene [7,8]. Mesothelin was identified as a cell surface antigen recognized by the monoclonal antibody K1 in human mesotheliomas and ovarian carcinomas [9–11]; MPF was independently identified in the culture supernatant of a human pancreatic carcinoma cell line, HPC-Y5 [12]. Human Mesothelin/MPF is derived from a common 71 kDa precursor [8,11]. The precursor protein is cleaved by a furin-like protease, and a 31 kDa NH_2-terminal peptide (MPF) is released into the extracellular

Abbreviations: PanIN, pancreatic intraepithelial neoplasias; PDA, pancreas ductal adenocarcinoma; AxCANCre, Cre recombinase-carrying adenovirus; TEF-1, transcription enhancer factor-1

* Corresponding author. Address: Nanotoxicology Project, Nagoya City University Graduate School of Medical Sciences, 1 Kawasumi, Mizuho-cho, Mizuho-ku, Nagoya 467-8601, Japan. Fax: +81 52 853 8996.
E-mail address: htsuda@med.nagoya-cu.ac.jp (H. Tsuda).

0006-291X/$ - see front matter © 2009 Elsevier Inc. All rights reserved.
doi:10.1016/j.bbrc.2009.10.019

space, leaving a 40 kDa COOH-terminal peptide (Mesothelin) attached to the cell surface by a GPI-anchor [9]. To avoid confusion, we refer to the rat Erc protein and its human homolog as Erc/Mesothelin. Erc/Mesothelin is expressed in ovary and pancreas carcinoma tissue in humans [13–15] and can be used as a marker for PDA [15]. Recently, we developed a novel sandwich ELISA system for serum Erc/Mesothelin [16–19]. Using this serum assay system, the level of Erc/Mesothelin was found to be higher in samples from mesothelioma patients than in samples from subjects without pancreas lesions [16,17]. In the present study we report the use of Erc/Mesothelin as a reliable serum marker for pre-symptomatic, premalignant pancreas lesions in *ras* Tg rats.

Materials and methods

Animals. Male Hras^{G12V} transgenic (Hras250) rats were bred with female Sprague–Dawley rats by CLEA Japan Inc. (Tokyo, Japan) as previously reported [4]. Routine genotyping of Hras250 rats was performed using the primers 5′-TCGTGCTTTACGGTATCGCCGCTCCC GATT-3′ and 5′-GATCTGCTCCCTGTACTGGTGG-3′. For the generation of transgenic rats conditionally expressing human Kras^{G12V}, 3× hemagglutinin (HA) tagged Kras^{G12V} cDNA was subcloned into the SacI/KpnI site of pCALNL5 (DNA Bank, RIKEN BioResource Center, Ibaraki, Japan). The purified cassette was injected into the pronuclei of Sprague–Dawley rats (CLEA Japan, Tokyo, Japan) as previously reported [4,20]. Two lines were established (Kras301 and Kras327). In this study, we used the Kras327 line. Routine genotyping of Kras327 rats was performed using the primers 5′-TCTGGATCAAATCCGAAC GC-3′ and 5′-TGACCTGCTGTGTCGAGAAT-3′. Rats were maintained in plastic cages in an air-conditioned room with a 12-h light/12-h dark cycle. The experiments were conducted according to the 'Guidelines for Animal Experiments of the Nagoya City University Graduate School of Medical Sciences'.

Tumor induction and pathological examination. AxCANCre was amplified in HEK293 cells and then purified using Vivapure Adenopack (Vivascience, Hannover, Germany). The titer of the adenovirus

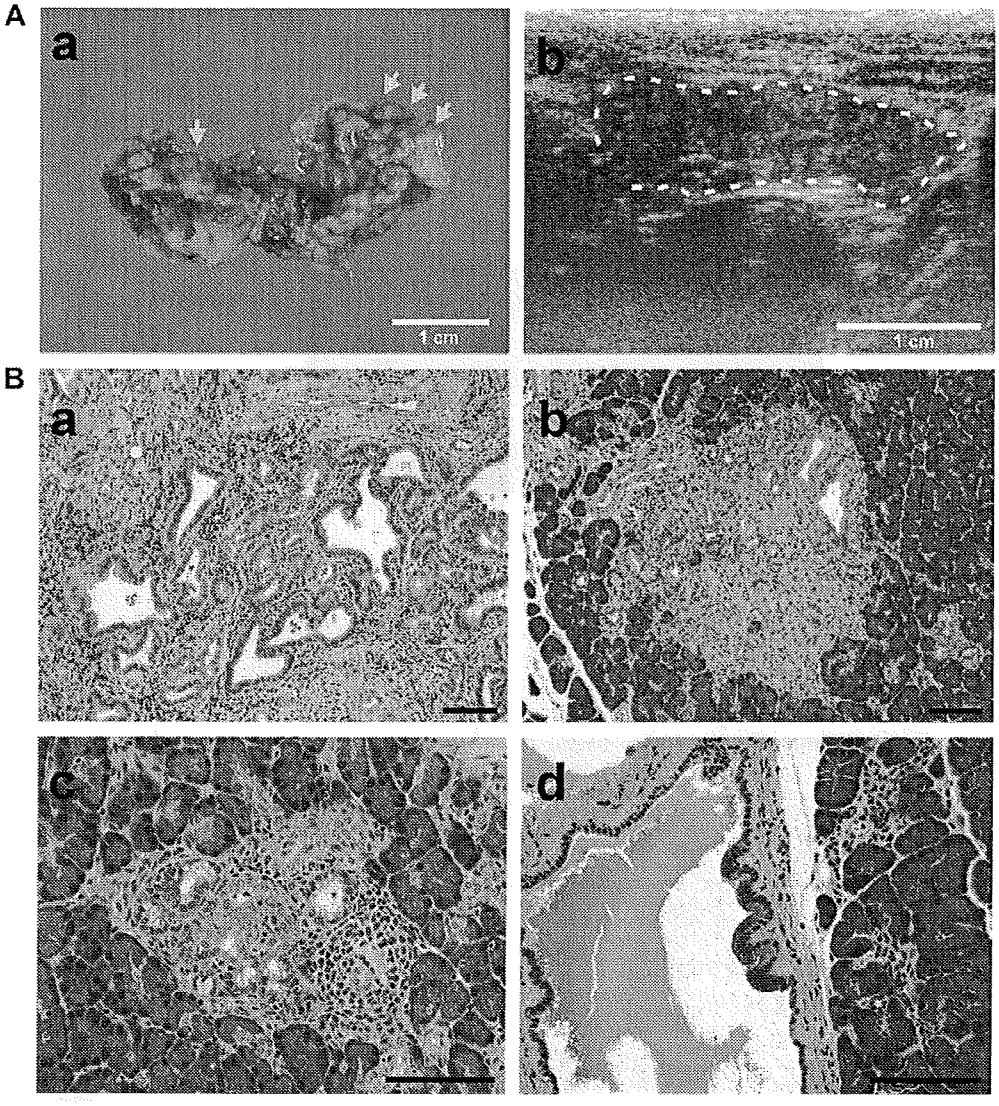

Fig. 1. Pancreas tumors developed in *ras* Tg rats. Animals were killed 3–4 weeks after injection of recombinant AxCANCre into the pancreas of adult *ras* Tg rats. (A) Macroscopic appearance of the pancreas with advanced multiple tumors (arrows) in an Hras250 rat (a). At this stage, multiple tumor nodules can be visualized by ultrasound image analysis (inside broken line) (b). (B) Histological appearance of pancreatic lesions. Large carcinoma (a), small carcinomas (b,c) and a PanIN-1a like lesion with slightly atypical duct epithelium (d). (a,b) are in Hras250 rats and (c) and (d) are grossly invisible small lesions in Kras327 rats. Bars = 100 μm.

Table 1
Microarray data: list of up-regulated genes encoding secreted proteins.

Gene	Accessions	Description	Expression level (tumor/control)
Mmp7	NM_012864	Matrix metalloproteinase-7	18.2
Tf	NM_001013110	Transferrin	14.4
Ctgf	NM_022266	Connective tissue growth factor	14.3
Cx3cl1	NM_134455	Chemokine (C-X3-C motif) ligand 1	7.7
Msln	NM_031658	Erc/Mesothelin	7.4
Lcn2	NM_130741	Lipocalin 2	7.0
Mmp2	U65656	Gelatinase A	6.0
Col18a1	XM_241632	Procollagen, type XVIII, alpha 1	5.5
Mgp	NM_012862	Matrix Gla protein	5.2
Sdc1	NM_013026	Syndecan 1	4.8

was determined using a rapid titer kit (Clontech, Mountain View, CA). Pancreas tumors were induced as described previously [4]. Ultrasound images were acquired using a microimaging system (EUB-8500, Hitachi Medical Corp., Tokyo, Japan). The pancreas was frozen in liquid nitrogen for RNA assays, or fixed in phosphate-buffered 10% formalin and processed for histological observation. Primary antibody anti-rat-C-ERC/Mesothelin (306) (IBL, Gunma, Japan) was used, and staining was performed using Vectastain ABC kits (Vector Laboratories, Burlingame, CA).

Tumors other than PDA were induced by chemical carcinogens, diethylnitrosamine (DEN) for liver cell tumor, *N*-butyl-*N*-(4-hydroxybutyl)nitrosamine (BBN) for bladder tumor, 7,12-dimethylbenz[a]anthracene (DMBA) for mammary tumor, *N*-bis(2-hydroxypropyl)nitrosamine (DHPN) for lung, kidney and thyroid tumor, and DMBA–12-*O*-tetradecanoylphorbol 13-acetate (TPA) for skin tumor.

Establishment of a rat pancreas cell line and Erc/Mesothelin analysis. A pancreas carcinoma cell line was established from a pancreas tumor from an Hras250 rat. The pancreas tumor tissue was placed in RPMI1640 medium at 4 °C. The tumor was diced into 1–2 mm^3 pieces and transplanted to NOD-SCID mice. Three months after transplantation, the tumor grew and reached a size of 10 mm in diameter. Tumor tissues were trimmed of fat and necrotic portions and minced with scalpels. The tissue pieces were transferred to 60-

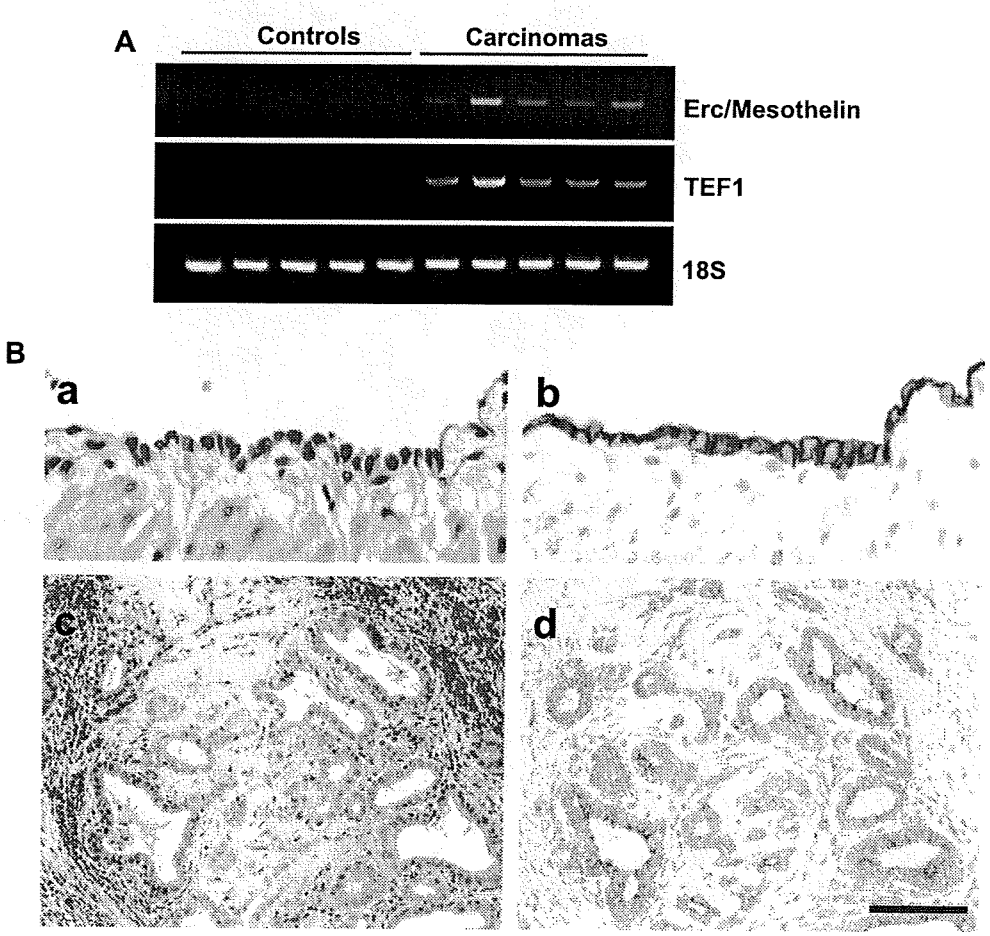

Fig. 2. Expression of Erc/Mesothelin in pancreatic lesions. (A) RT-PCR for Erc/Mesothelin and TEF-1 of normal pancreas and carcinomas in Hras250 rats. Each lane represent RNA prepared from an individual rat. 18S ribosome serves as an RNA control. (B) Immunostaining of Erc/Mesothelin in the mesothelium (a,b) and PDA (c,d) lesions. The antibody is more dense in the apical border. (a,c), H&E staining; (b,d), Erc/Mesothelin staining. Bar = 100 μm.

mm culture dishes at 10–15 fragments/dish. Fibroblasts were removed mechanically and by trypsinization (trypsin, 0.05%; EDTA, 0.02%). The cells were cultured on dishes. The established cell line was maintained in DMEM/Keratinocyte-SFM (Gibco, Grand Island, NY) containing 10% FCS. The cells were seeded in 1 ml of medium at a cell density of 10^5 cells/35-mm plate and cultured for 2 days. Cells were harvested and the cultured supernatant collected.

The tumor cells (1×10^6 or 1×10^7) were transplanted subcutaneously into 6 week old male NOD-SCID mice (Charles River Laboratories Japan, Inc., Yokohama, Japan). After 5 weeks of transplantation, the tumor was weighed and serum was collected for analysis of Erc/Mesothelin.

RT-PCR. Total RNA was isolated using ISOGEN (Nippon Gene, Toyama, Japan). A total of 450 ng of total RNA (from control pancreas and tumor samples) was reverse-transcribed using Superscript III Reverse Transcriptase with Random primers (Invitrogen, Carlsbad, CA). Reverse-transcription reaction mixtures were diluted 1:100 and 2 μl was used for PCR. The following primers were used: *Erc/Mesothelin*, 5′-ACCGTTGACTTTGCCAGTCT-3′ and 5′-TGCATCCGTCTCAC TCACTT-3′; *TEF-1*, 5′-ATTCTTACAGCGACCCGTTG-3′ and 5′-TGCTCCA TGCTCACTATTCG-3′; ribosome 18S, 5′-GTTGGTGGAGCGATTTGTCT-3′ and 5′-GGCCTCACTAAACCATCCAA-3′.

Serum test. The serum level of Erc/Mesothelin was quantified by the ELISA system (Code No.27765, Rat N-ERC/Mesothelin Assay Kit, IBL, Gunma, Japan) described previously [19]. Serum levels of CA19-9, Dupan-2, and SPan-1 were assayed by SRL, Inc. (Tokyo, Japan).

Microarray analysis. For gene microarray analysis, mRNA was isolated from total RNA (pooled sample from five animals) using a "Poly(A)+ Isolation Kit from total RNA" (Nippon Gene) according to the manufacturer's instructions. Microarray analysis was performed by Hokkaido System Science Co., Ltd. (Sapporo, Japan) using Whole Rat Oligo Microarray (Agilent Technologies, Inc., Santa Clara, CA). The experiments were performed twice by switching dyes reciprocally.

Results

Ras Tg rats, 10–30 weeks of age, were killed 3–4 weeks after injection of recombinant AxCANCre into the pancreatic duct via the common bile duct. Many grossly visible whitish tumor nodules were observed throughout the pancreas in both types of *ras* Tg rats, although they were slightly fewer in number in the Kras327 lines. Pancreas tumors developed in all *ras* Tg rats without any relationship to their age. These multiple tumors can be detected by ultrasound imaging (Fig. 1A). Histological examination showed that these nodules were adenocarcinomas with a variable amount of fibrotic tissue proliferation, some showing desmoplastic morphology. Neoplastic lesions were not found in any other organs. Carcinomas caused destruction of pancreas tissue by infiltrative growth, however, remote metastasis was not observed. Representative cases of an advanced carcinoma, early small carcinomas, and a PanIN-1a lesion are shown in Fig. 1B. These pancreas lesions were positive for alucian blue, cytokeratins 19 and 7, cyclooxigenase-2 (COX-2), matrix metalloproteinase-7 (MMP-7), epidermal growth factor (EGF) and EGFR, but negative for amylase, as reported previously [4].

Serum CA19-9, Dupan-2, and SPan-1, which are currently available serum markers for human pancreas cancer, were not detected in pancreas tumor-bearing rats using human antibodies. We performed a comprehensive and global analysis of over 40,000 genes to find diagnosis markers to detect rat PDA. Pancreas tumor tissue with frank ductal adenocarcinomas from Hras250 rats was subjected to microarray analysis. Table 1 lists the top 10 up-regulated genes encoding secreted proteins; secreted proteins are of particular interest for their potential diagnostic value. Our microarray analysis indicated that Erc/Mesothelin was overexpressed 7.4-fold in pancreas carcinoma tissue compared to pancreata of wild type littermates. Importantly, a previous report showed that overexpression of Erc/Mesothelin was identified in the majority of pancreas carcinomas in humans [15]. Therefore, we focused on the preferential expression of Erc/Mesothelin in PDA of *ras* Tg rats.

The expression level of the Erc/Mesothelin gene was confirmed by RT-PCR. Erc/Mesothelin gene expression in pancreatic carcinoma was higher than in the pancreata of wild type littermates (Fig. 2A). Recently, Hucl et al. reported that the presence of transcription enhancer factor (TEF)-1 was required for high cancer-specific expression of Erc/Mesothelin [21]. Similarly, we found that the mRNA expression level of TEF-1 was higher in pancreatic carcinomas than in pancreas tissue from wild type littermates (Fig. 2A). Finally, immunohistochemical studies showed higher expression of Erc/Mesothelin in small carcinoma lesions as compared to surrounding normal tissue (Fig. 2B).

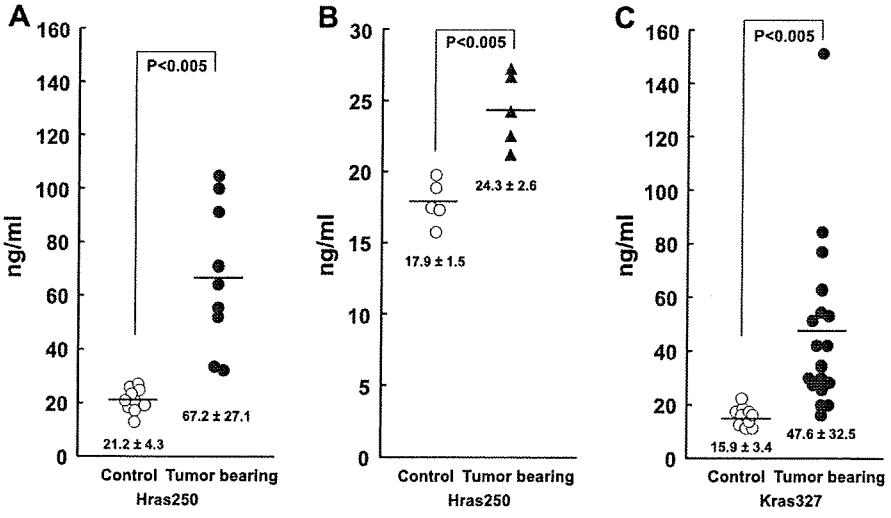

Fig. 3. Levels of N-ERC in rats bearing neoplastic lesions. (A) The serum levels of N-ERC in Hras250 rats bearing multiple pancreas ductal carcinomas was significantly higher than in untreated wild type control littermates ($P < 0.005$). (B) Serum N-ERC in Hras250 rats with early small carcinomas was also significantly higher than in untreated wild type control littermates ($P < 0.005$). The early lesions, not visible by eye, were detected microscopically. (C) The serum level of N-ERC in Kras327 rats bearing multiple pancreas ductal carcinomas was significantly higher than in untreated Kras327 control rats ($P < 0.005$). All animals were sacrificed 3 weeks after the AxCANCre injection.

We initially assayed the serum levels of the NH_2-terminal secretory form of Erc/Mesothelin (N-ERC) in Hras250 rats with pancreas carcinomas and in wild type littermates without pancreas carcinomas (Fig. 3). N-ERC levels in Hras250 rats bearing pancreas carcinomas was 67.2 ± 27.1 ng/ml (mean ± SD) (n = 9), whereas the levels in wild type Hras250 littermates was 21.2 ± 4.3 ng/ml (n = 10) (Fig. 3A). These results confirmed our ability to detect differences in serum N-ERC levels in animals in which Erc/Mesothelin was expressed at high (pancreas tumor-bearing Hras250 rats) and low (wild type littermates without pancreas tumors) levels.

To determine whether elevated levels of N-ERC can be detected in rats with early stage lesions, serum N-ERC levels in Hras250 rats with grossly normal-looking pancreas containing microscopic ductal adenoma/adenocarcinoma lesions were compared to untreated wild type littermates. The levels of N-ERC in rats with early lesions was 24.3 ± 2.6 ng/ml (n = 5) whereas the level in their untreated littermates was 17.9 ± 1.5 ng/ml (n = 5) (P < 0.005) (Fig. 3B). We then measured the levels of N-ERC in untreated Hras250 rats and in Hras250 rats treated with control adenovirus vector. The serum levels of N-ERC were the same in untreated Hras250 rats and Hras250 rats treated with control vector, and these levels were the same or somewhat lower than the levels in the Hras250 wild type littermates (data not shown). These results indicate that in the Hras250 animal model, increased N-ERC can be detected in the serum of animals with pre-malignant lesions.

Next we assayed N-ERC levels in the Kras transgenic rats. The level of N-ERC in tumor-bearing Kras327 rats was 47.6 ± 32.5 ng/ml (n = 18) whereas those of untreated Kras327 rats was 15.9 ± 3.4 ng/ml (n = 10) (P < 0.005) (Fig. 3C). In all serum samples, the COOH-terminal form of Erc/Mesothelin (C-ERC) was undetectable.

Since PDA lesions frequently include variable amounts of mesenchymal tissue, an increase in tumor associated mesothelial cells could cause an increase in serum N-ERC levels. We therefore evaluated the levels in a pancreas carcinoma cell line (designated 634NOD) derived from a pancreas ductal adenocarcinoma from an Hras250 rat. 634NOD cells were implanted subcutaneously into the flank of NOD-SCID mice, and the resulting tumor was positive for cytokeratins 19 and 7, markers of pancreatic duct (histology not shown). In tissue culture, the 634NOD cells expressed Erc/Mesothelin (Fig. 4A), and N-ERC could be detected in the culture supernate (389.4 ± 11.7 ng/ml) (Fig. 4B). C-ERC levels were extremely low to undetectable (Fig. 4B). Taken together, the results reported here clearly indicate that the elevated N-ERC detected in the serum of transgenic rats bearing pre-malignant pancreatic lesions was derived from these lesions.

To determine whether serum levels of N-ERC correlated with tumor size, we assayed N-ERC levels in NOD-SCID mice with transplanted 634NOD cells. N-ERC was detected in the serum of these mice. Increase in the serum level of N-ERC correlated with increased with tumor size (R = 0.918, P < 0.001) (Fig. 4C). This result indicates a causal relationships between serum level of N-ERC and tumor size.

Serum N-ERC levels in rats with tumors such as bladder transitional cell tumors, liver cell tumors, lung, kidney, thyroid, mammary, prostate, and skin tumors induced by chemical carcinogens were not significantly elevated compared to their respective controls (data not shown).

Discussion

For the purpose of developing methods to detect early cancer lesions, preferably at a preclinical stage, use of an appropriate animal model is advantageous because of the experimental availability of early lesions. To the best of our knowledge, available serum

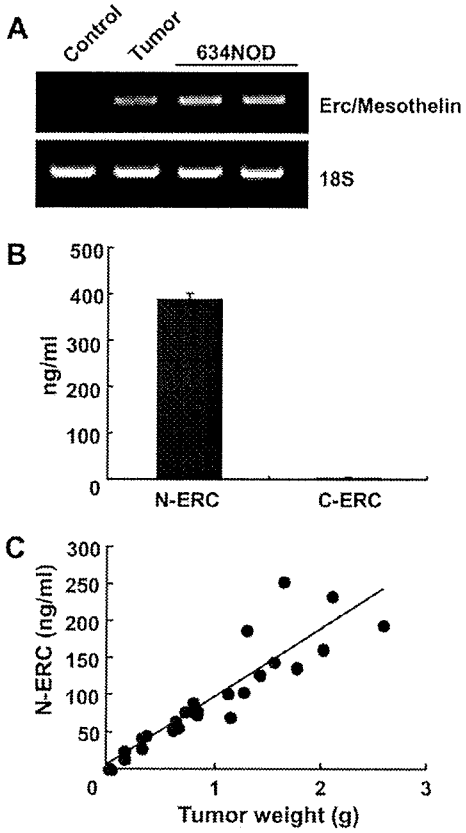

Fig. 4. The Erc/Mesothelin gene was expressed in an established pancreas ductal carcinoma cell line. (A) RT-PCR for Erc/Mesothelin in a pancreas carcinoma cell line. Control: pancreas from empty vector treated Hras250 rats (pooled sample from five animals). Tumor: pancreas carcinomas from AxCANCre injected Hras250 rats (pooled sample from five animals). 634NOD: pancreas carcinoma cell line (established from a pancreas tumor from an AxCANCre injected Hras250 rat). (B) Levels of N- and C-terminal derived Erc/Mesothelin (N-ERC and C-ERC, respectively) protein in the culture medium from a pancreas carcinoma cell line. The precursor protein is cleaved by a furin-like protease: a 31 kDa NH_2-terminal half (N-ERC) is released into the extracellular space, leaving the 40 kDa COOH-terminal half (Mesothelin) attached to the cell surface by a GPI-anchor. (C) Serum level of N-ERC in 634NOD transplanted NOD-SCID mice. The serum level of N-ERC correlated with increased tumor weight (R = 0.918, P < 0.001).

markers for cancer in animal models are limited to prostate cancer [22]. Antibodies for pancreas tumor associated human serum markers CA19-9, Dupan-2 and SPan-1 recognize carbohydrate chains, such as Sialyl Le^a, Sialyl Le^c. In this study, we found that serum levels of CA19-9, Dupan-2, and SPan-1 were below detectable levels in pancreas tumor-bearing rats regardless of stage. Cross-reactivity of these antibodies for human tumor carbohydrate antigen in rodents has not been clearly demonstrated. We have established rat models of pancreas ductal carcinomas. These models use a human $Hras^{G12V}$ (Hras250) [4] or a human $Kras^{G12V}$ (Kras327) oncogene under the control of the Cre/loxP system to induce cancerous lesions. Neoplastic lesions in the *ras* Tg rats exhibited morphological and biological similarities to those observed in human pancreas lesions. Using these models, we showed that preclinical pancreas ductal neoplasms can be diagnosed by measuring Erc/Mesothelin in the serum (Fig. 3).

N-ERC is a 31 kDa protein that forms the N-terminal fragment of the full-length 71 kDa Erc/Mesothelin protein and is secreted into the blood of mesothelioma patients. The ELISA system used in this study was originally used for the detection of N-ERC in the serum of mesothelioma patients [16]. The system was also used to detect N-ERC in the serum of Eker rats [18,23,24], and it

clearly worked in this study to detect higher levels of N-ERC in the serum of pancreas tumor-bearing rats. The expression levels of TEF-1 mRNA in pancreas tumors correlated with that of Erc/Mesothelin in tumor tissue and N-ERC in the serum. Since Erc/Mesothelin mRNA was found at relatively low levels in the normal rat pancreas, increased serum levels of N-ERC appear to be specific for pancreas carcinomas in the *ras* Tg rat models.

Many human pancreas cancer cell lines express Erc/Mesothelin [12,21,25]. N-ERC was detected in the supernatants of cultured human pancreas cancer cells, and correlated with the expression levels of Erc/Mesothelin [25]. Although there was no significant difference in serum N-ERC concentrations between pancreas cancer patients and healthy control groups [25], Erc/Mesothelin is frequently expressed in ductal carcinoma, but not in normal pancreas or chronic pancreatitis [15,25–27]. Thus, Erc/Mesothelin expression can be found in both human and rat pancreas ductal adenocarcinoma.

Previous immunohistochemical studies showed that expression of Mesothelin is found in most epithelioid mesothelioma, nonmucinous carcinomas of the ovary, adenocarcinomas of the pancreas, some breast, uterus, colorectal and lung adenocarcinomas, but not in carcinomas of the prostate, kidney, liver, thyroid, or bladder in humans [13,27–29]. In line with human data, although we have not thoroughly examined all the different tumors induced by chemical carcinogens, available data indicates that increase in serum N-ERC level is relatively specific for PDA in rats.

One advantage of using rats is that their relatively large organ size facilitates surgical procedures. In this rat model, serum levels of N-ERC can be used for the identification of early neoplastic lesions, even in preclinical stages, and also for monitoring the further progression of carcinogenesis. The model may also be used to screen for candidate chemotherapeutic agents, which could be evaluated for human use. Furthermore, serum N-ERC may prove useful for the diagnosis of pre-symptomatic lesions for human mesothelioma or ovary cancer patients.

Acknowledgments

We thank Dr. T. Sugimura (National Cancer Center) for his valuable advice, Dr. T. Shirai (Nagoya City University) for his assistance with histological specimen preparation and advice for histological examination, Drs. M. Wei (Osaka City University), S. Tamano (DIMS institute of Medical Science), S. Yamashita and T. Ushijima (National Cancer Center) for rat serum provision, and Dr. J. Miyazaki (Osaka University) for the CAG promoter provision. We also thank Y. Morita, S. Ariji, K. Ohmi and Y. Terashima, training students, for their enthusiastic assistance with establishment of the transgenic rats.

This work was supported in part by the Grant-in-Aid for Scientific Research (C) from Japan Society for the Promotion of Science, the Grant-in-Aid for Cancer Research (15-2, 16-13, 17S-6, 20S-8), the Grant-in-Aid for Research on Nanotechnical Medical (H19-nano-ippan-014), the Grant-in-Aid for Research on Risk of Chemical Substances (H18-kagaku-ippan-007, H19-Kagaku-Ippan-006) from the Ministry of Health, Labour, and Welfare of Japan, and Grant-in-Aid for Food Safety Commission, Japan (051).

References

[1] H.G. Beger, B. Rau, F. Gansauge, B. Poch, K.H. Link, Treatment of pancreatic cancer: challenge of the facts, World J. Surg. 27 (2003) 1075–1084.
[2] A. Jemal, R. Siegel, E. Ward, T. Murray, J. Xu, M.J. Thun, Cancer statistics, 2007, CA Cancer J. Clin. 57 (2007) 43–66.
[3] E.P. DiMagno, H.A. Reber, M.A. Tempero, AGA technical review on the epidemiology, diagnosis, and treatment of pancreatic ductal adenocarcinoma, Am. Gastroenterol. Assoc. Gastroenterol. 117 (1999) 1464–1484.
[4] S. Ueda, K. Fukamachi, Y. Matsuoka, N. Takasuka, F. Takeshita, A. Naito, M. Iigo, D.B. Alexander, M.A. Moore, I. Saito, T. Ochiya, H. Tsuda, Ductal origin of pancreatic adenocarcinomas induced by conditional activation of a human Ha-ras oncogene in rat pancreas, Carcinogenesis 27 (2006) 2497–2510.
[5] O. Hino, E. Kobayashi, M. Nishizawa, Y. Kubo, T. Kobayashi, Y. Hirayama, S. Takai, Y. Kikuchi, H. Tsuchiya, K. Orimoto, K. Kajino, T. Takahara, H. Mitani, Renal carcinogenesis in the Eker rat, J. Cancer Res. Clin. Oncol. 121 (1995) 602–605.
[6] Y. Yamashita, M. Yokoyama, E. Kobayashi, S. Takai, O. Hino, Mapping and determination of the cDNA sequence of the Erc gene preferentially expressed in renal cell carcinoma in the Tsc2 gene mutant (Eker) rat model, Biochem. Biophys. Res. Commun. 275 (2000) 134–140.
[7] K. Chang, I. Pastan, Molecular cloning of mesothelin, a differentiation antigen present on mesothelium, mesotheliomas, and ovarian cancers, Proc. Natl. Acad. Sci. USA 93 (1996) 136–140.
[8] T. Kojima, M. Oh-eda, K. Hattori, Y. Taniguchi, M. Tamura, N. Ochi, N. Yamaguchi, Molecular cloning and expression of megakaryocyte potentiating factor cDNA, J. Biol. Chem. 270 (1995) 21984–21990.
[9] K. Chang, L.H. Pai, J.K. Batra, I. Pastan, M.C. Willingham, Characterization of the antigen (CAK1) recognized by monoclonal antibody K1 present on ovarian cancers and normal mesothelium, Cancer Res. 52 (1992) 181–186.
[10] K. Chang, I. Pastan, M.C. Willingham, Isolation and characterization of a monoclonal antibody, K1, reactive with ovarian cancers and normal mesothelium, Int. J. Cancer 50 (1992) 373–381.
[11] K. Chang, I. Pastan, Molecular cloning and expression of a cDNA encoding a protein detected by the K1 antibody from an ovarian carcinoma (OVCAR-3) cell line, Int. J. Cancer 57 (1994) 90–97.
[12] N. Yamaguchi, K. Hattori, M. Oh-eda, T. Kojima, N. Imai, N. Ochi, A novel cytokine exhibiting megakaryocyte potentiating activity from a human pancreatic tumor cell line HPC-Y5, J. Biol. Chem. 269 (1994) 805–808.
[13] N. Scholler, N. Fu, Y. Yang, Z. Ye, G.E. Goodman, K.E. Hellstrom, I. Hellstrom, Soluble member(s) of the mesothelin/megakaryocyte potentiating factor family are detectable in sera from patients with ovarian carcinoma, Proc. Natl. Acad. Sci. USA 96 (1999) 11531–11536.
[14] C.D. Hough, C.A. Sherman-Baust, E.S. Pizer, F.J. Montz, D.D. Im, N.B. Rosenshein, K.R. Cho, G.J. Riggins, P.J. Morin, Large-scale serial analysis of gene expression reveals genes differentially expressed in ovarian cancer, Cancer Res. 60 (2000) 6281–6287.
[15] P. Argani, C. Iacobuzio-Donahue, B. Ryu, C. Rosty, M. Goggins, R.E. Wilentz, S.R. Murugesan, S.D. Leach, E. Jaffee, C.J. Yeo, J.L. Cameron, S.E. Kern, R.H. Hruban, Mesothelin is overexpressed in the vast majority of ductal adenocarcinomas of the pancreas: identification of a new pancreatic cancer marker by serial analysis of gene expression (SAGE), Clin. Cancer Res. 7 (2001) 3862–3868.
[16] K. Shiomi, H. Miyamoto, T. Segawa, Y. Hagiwara, A. Ota, M. Maeda, K. Takahashi, K. Masuda, Y. Sakao, O. Hino, Novel ELISA system for detection of N-ERC/mesothelin in the sera of mesothelioma patients, Cancer Sci. 97 (2006) 928–932.
[17] K. Shiomi, Y. Hagiwara, K. Sonoue, T. Segawa, K. Miyashita, M. Maeda, H. Izumi, K. Masuda, M. Hirabayashi, T. Moroboshi, T. Yoshiyama, A. Ishida, Y. Natori, A. Inoue, M. Kobayashi, Y. Sakao, H. Miyamoto, K. Takahashi, O. Hino, Sensitive and specific new enzyme-linked immunosorbent assay for N-ERC/Mesothelin increases its potential as a useful serum tumor marker for mesothelioma, Clin. Cancer Res. 14 (2008) 1431–1437.
[18] M. Nakaishi, K. Kajino, M. Ikesue, Y. Hagiwara, M. Kuwahara, H. Mitani, Y. Horikoshi-Sakuraba, T. Segawa, S. Kon, M. Maeda, T. Wang, M. Abe, M. Yokoyama, O. Hino, Establishment of the enzyme-linked immunosorbent assay system to detect the amino terminal secretory form of rat Erc/Mesothelin, Cancer Sci. 98 (2007) 659–664.
[19] Y. Hagiwara, Y. Hamada, M. Kuwahara, M. Maeda, T. Segawa, K. Ishikawa, O. Hino, Establishment of a novel specific ELISA system for rat N- and C-ERC/mesothelin. Rat ERC/mesothelin in the body fluids of mice bearing mesothelioma, Cancer Sci. 99 (2008) 666–670.
[20] M. Asamoto, T. Ochiya, H. Toriyama-Baba, T. Ota, T. Sekiya, M. Terada, H. Tsuda, Transgenic rats carrying human c-Ha-ras proto-oncogenes are highly susceptible to *N*-methyl-*N*-nitrosourea mammary carcinogenesis, Carcinogenesis 21 (2000) 243–249.
[21] T. Hucl, J.R. Brody, E. Gallmeier, C.A. Iacobuzio-Donahue, I.K. Farrance, S.E. Kern, High cancer-specific expression of mesothelin (MSLN) is attributable to an upstream enhancer containing a transcription enhancer factor dependent MCAT motif, Cancer Res. 67 (2007) 9055–9065.
[22] I.V. Huizen, G. Wu, M. Moussa, J.L. Chin, A. Fenster, J.C. Lacefield, H. Sakai, N.M. Greenberg, J.W. Xuan, Establishment of a serum tumor marker for preclinical trials of mouse prostate cancer models, Clin. Cancer Res. 11 (2005) 7911–7919.
[23] O. Hino, Multistep renal carcinogenesis in the Eker (Tsc 2 gene mutant) rat model, Curr. Mol. Med. 4 (2004) 807–811.
[24] M. Maeda, O. Hino, Molecular tumor markers for asbestos-related mesothelioma: serum diagnostic markers, Pathol. Int. 56 (2006) 649–654.
[25] K. Inami, K. Kajino, M. Abe, Y. Hagiwara, M. Maeda, M. Suyama, S. Watanabe, O. Hino, Secretion of N-ERC/mesothelin and expression of C-ERC/mesothelin in human pancreatic ductal carcinoma, Oncol. Rep. 20 (2008) 1375–1380.
[26] R. Hassan, Z.G. Laszik, M. Lerner, M. Raffeld, R. Postier, D. Brackett, Mesothelin is overexpressed in pancreaticobiliary adenocarcinomas but not in normal pancreas and chronic pancreatitis, Am. J. Clin. Pathol. 124 (2005) 838–845.
[27] N.G. Ordonez, Application of mesothelin immunostaining in tumor diagnosis, Am. J. Surg. Pathol. 27 (2003) 1418–1428.
[28] N.G. Ordonez, Value of mesothelin immunostaining in the diagnosis of mesothelioma, Mod. Pathol. 16 (2003) 192–197.
[29] H.F. Frierson Jr., C.A. Moskaluk, S.M. Powell, H. Zhang, L.A. Cerilli, M.H. Stoler, H. Cathro, G.M. Hampton, Large-scale molecular and tissue microarray analysis of mesothelin expression in common human carcinomas, Hum. Pathol. 34 (2003) 605–609.

Cancer Science
The official journal of the Japanese Cancer Association JCA

Mature acinar cells are refractory to carcinoma development by targeted activation of Ras oncogene in adult rats

Hajime Tanaka,[1] Katsumi Fukamachi,[2] Mitsuru Futakuchi,[2] David B. Alexander,[2] Ne Long,[2] Shojiro Tamamushi,[4] Kohtaro Minami,[5] Susumu Seino,[5] Hirotaka Ohara,[1] Takashi Joh[1] and Hiroyuki Tsuda[2,3,6]

[1]Departments of Gastroenterology and Metabolism, [2]Molecular Toxicology and [3]Nanotoxicology Project, Nagoya City University Graduate School of Medical Sciences, Nagoya; [4]CLEA Japan Inc., Shizuoka; [5]Division of Cellular and Molecular Medicine Kobe University Graduate School of Medicine, Kobe, Japan

(Received July 20, 2009/Revised October 8, 2009/Accepted October 13, 2009/Online publication November 16, 2009)

Pancreatic ductal adenocarcinoma (PDA) is one of the most debilitating malignancies in humans. A thorough understanding of the cytogenesis of this disease will aid in establishing successful treatments. We have developed an animal model which uses adult $Hras^{G12V}$ and $Kras^{G12V}$ transgenic rats in which oncogene expression is regulated by the Cre/loxP system and neoplastic lesions are induced by injection of adenovirus-expressing Cre recombinase. When adenovirus with Cre recombinase under the control of the CMV enhancer/chicken β-actin (CAG) promoter (Ad-CAG-Cre) is injected into the pancreatic duct of these animals, pancreatic neoplasias develop. Pathologically, the origin of these lesions is duct, intercalated duct, and centroacinar cells, but not acinar cells. The present study was undertaken to test the effect of acinar cell-specific oncogenic *ras* expression. Adult transgenic rats were injected with adenovirus with Cre recombinase under the control of the acinar cell-specific promoters amylase (Ad-Amy-Cre) and elastase-1 (Ad-Ela-Cre) or under the control of the non-specific CAG promoter. Injection of either Ad-Amy-Cre or Ad-Ela-Cre into the pancreatic ducts of transgenic animals in which oncogenic *Kras* is tagged with hemagglutinin (HA), HA-$Kras^{G12V}$ rats resulted in expression of oncogenic *ras* in acinar cells but not in duct, intercalated duct, or centroacinar cells. Notably, injected animals did not develop any observable proliferative or neoplastic lesions. In marked contrast, injection of Ad-CAG-Cre resulted in pancreatic cancer development within 4 weeks. These results indicate that adult acinar cells are refractory to Ras oncogene activation and do not develop neoplasia in this model. (*Cancer Sci* 2010; 101: 341–346)

Pancreatic ductal adenocarcinoma (PDA) is a highly lethal disease, which is usually diagnosed in an advanced state. Most patients die within 1 year of diagnosis, [1] and the 5-year survival rate is <5%.[2] Understanding of the cytogenesis of PDA offers new directions for targeted therapeutic approaches to combat this disease.

Previously, we reported on an animal model in which pancreatic neoplasia was induced in adult $Hras^{G12V}$ transgenic rats by injection of adenovirus with Cre recombinase under the control of the CMV enhancer/chicken β-actin (CAG) promoter into the pancreatic duct.[3] In these animals, it was shown that duct, intercalated duct, centroacinar, and acinar cells were all infected with the adenovirus, but induced pre-neoplastic and neoplastic lesions were shown to express only duct cell-specific characteristics and not acinar cell-specific characteristics. Moreover, proliferative lesions were not observed in acinar cells. Therefore, we hypothesized that PDA does not develop from adult pancreatic acinar cells in this model.

The present study was undertaken to directly test the capability of mature acinar cells to develop into a neoplastic lesion. Transgenic rats with an Hras or hemagglutinin (HA)-tagged Kras oncogene were injected with Cre recombinase expressing adenoviruses in which Cre expression was under the control of promoters specifically active in acinar cells. Mature acinar cells in injected rats did express active Ras proteins, but did not develop any proliferative or neoplastic lesions.

Materials and Methods

Generation of transgenic rats. For the generation of transgenic rats conditionally expressing human $Kras^{G12V}$ we first made a cDNA fragment encoding the human $Kras4B^{G12V}$ with a 3× HA tag sequence at its 5′ end (HA-$Kras^{G12V}$). The HA-$Kras^{G12V}$ cDNA was subcloned into the SacI/KpnI site of pCALNL5 (DNA Bank, RIKEN Bio Resource Center, Ibaraki, Japan)[4,5] to produce pCALNLHAKras. pCALNLHAKras was digested with SalI/HindIII. The purified cassette (Fig. 1A) was injected into the pronuclei of Sprague–Dawley rats (CLEA Japan, Tokyo, Japan). Techniques used for the generation of transgenic rats were the same as those reported previously.[3,6] A total of 265 injected eggs were transplanted into pseudo-pregnant Sprague–Dawley rats. Of 37 potential transgenic rats screened, four male and one female rat were shown by PCR to carry the transgene. Transgenic founder rats were mated with Sprague–Dawley rats, and offspring were screened for the presence of the transgene by PCR analysis of genomic DNA isolated from tail biopsies at the age of 3 weeks. The following primers were used: 5′-TCTGGATCAAATCCGAACGC-3′, 5′-TGACCTGCTGTGTC-GAGAAT-3′. Two founder rats carrying a CALNLHA$Kras^{G12V}$ transgene transmittable to descendent generations (Kras301and Kras327) and two founder rats (Kras409 and Kras417) carrying a non-tagged $Kras^{G12V}$ transgene were established using the same cassette (data not shown). In this study, we used Kras301 and Kras327. Hras250 rats conditionally expressing human $Hras^{G12V}$ were generated as previously described. [3] They were maintained in plastic cages in an air-conditioned room with a 12-h light/12-h dark cycle. All experiments were conducted according to the Guidelines for Animal Experiments of the Nagoya City University Graduate School of Medical Sciences.

Preparation of adenovirus vectors. Adenoviruses in which either the mouse amylase-2 or the rat elastase-1 promoter drove the expression of Cre recombinase (Ad-Amy-Cre or Ad-Ela-Cre) (Fig. 1B) were prepared as described previously.[7] Recombinant adenovirus vectors carrying the *Cre* gene (Ad-CAG-Cre) (Fig. 1B) and empty adenovirus vector were prepared as described previously.[3] Recombinant adenovirus vectors were amplified in HEK-293 cells and then purified using Vivapure

[6]To whom correspondence should be addressed.
E-mail: htsuda@med.nagoya-cu.ac.jp

doi: 10.1111/j.1349-7006.2009.01410.x